



NTNU – Trondheim
Norwegian University of
Science and Technology

Fatigue Analysis and Design of Mooring Systems. Assessment and comparison of different methods.

Mohammad hasan Saidee

Marine Technology

Submission date: June 2015

Supervisor: Kjell Larsen, IMT

Norwegian University of Science and Technology
Department of Marine Technology



**NORWEGIAN UNIVERSITY OF SCIENCE AND TECHNOLOGY
DEPARTMENT OF MARINE TECHNOLOGY**

MASTER THESIS

SPRING 2015

**Fatigue Analysis and Design of Mooring Systems. Assessment and
Comparison of Different Analysis Methods**

Utmatting av ankerliner – vurdering og sammenligning av ulike designmetoder

Supervised by

Kjell Larsen

Submitted by

Mohammad Hasan Saidee

Preface

This project is carried out for the completion of my Master degree program in Marine Technology at Norwegian University of Science and Technology (NTNU) and represents the results of my studies from January to June 2015.

This thesis has been done under the supervision of Kjell Larsen from Statoil. I would like to thank him for his guidance and help throughout the whole thesis. His lecture notes and specially lectures on the black board during the project work were invaluable help to me for understanding mooring system and physical problems related to it.

A warm thank is also given to Vegard Øgård Aksnes and Pål Levold from MARINTEK for giving me guidance on modeling in SIMA. Learning SIMA software was really challenging at the beginning but with their help I managed to create the model and do post-processing successfully.

I would also like to thank Lasse Moldestad and Kai Roger Nilsen from Deep Sea Mooring for their valuable lectures on mooring analysis and sharing their practical knowledge in connection with mooring analysis task during project work.

Overall I am quite satisfied and pleased for choosing this project and learned a lot about mooring analysis and software tools related to it.

MTS, Trondheim

10th June 2015



Mohammad Hasan Saidee

MASTER THESIS SPRING 2015
for
Stud. tech. Mohammad Hasan Saidee

**Fatigue Analysis and Design of Mooring Systems. Assessment and
Comparison of Different Analysis Methods**

Utmatting av ankerliner – vurdering og sammenligning av ulike designmetoder

Background

The purpose of the mooring system is to keep a floating vessel safely at a required position. It normally consists of 8-16 mooring lines of heavy chain, steel wire ropes and/or synthetic polyester ropes connected to a seabed anchor.

During the past years, the requirements to the mooring and station keeping systems of mobile and permanent units have become more complex;

- The industry is moving into new frontiers (ultra-deep water down to 3000m depth and into arctic areas).
- There are more operations adjacent to other installations (flotel operations and tender support vessel operations).
- The new mobile units are becoming larger and many units are at the end of their lifetime.

In addition, mooring failure rate is unacceptably high. Some incidents have been multiple line failures, leading to vessel drifting. The investigations show a variety of direct causes covering both inaccurate design, bad quality in fabrication of mooring line components and insufficient fatigue resistance of components, in particular the mooring chain component.

This master thesis shall build on the work performed during the project work carried out autumn 2014, but the focus and content of this MSc is related to the fatigue design of mooring components according to the Fatigue Limit State (FLS) criteria.

Analysis methods for estimating ultimate mooring line tension can be divided into frequency domain (FD) methods and time domain (TD) methods. Using FD methods, the low frequency (LF) load effects and the wave frequency (WF) load effects are analyzed separately and then combined into characteristic values used in recipes for FLS design. The dynamic system describing the behavior of the vessel must be linearized and the dynamic tension ranges of line tensions are usually assumed to be statistically distributed according to the Rayleigh distribution. When using TD methods, all non-linearities in the dynamic system (stiffness and damping) and in the excitation may be taken into account. The result of TD simulations is time series of mooring line tensions. From these statistical distributions of tension cycles are normally estimated by rain flow counting techniques.

Scope of Work

- 1)
 - a) Describe the selected vessel (Åsgard A FPSO) in terms of main particulars, general layout and hydrodynamic properties. The description shall cover characteristics of wind forces, current forces, wave drift forces and first order motion RAOs.
 - b) Describe the FLS acceptance criteria (design fatigue factors (DFFs) and recipes) relevant for the Norwegian Continental Shelf (NCS).
- 2) Review relevant literature and describe the different aspects and differences of using FD and TD analysis methods for analysis of mooring line tension for a typical short term steady sea state. The software tools MIMOSA (FD) and SIMO/RIFLEX (TD) shall be used. Base case method for TD shall be a fully coupled approach.
- 3) Describe the design recipes and different analysis steps to be performed for a FLS design check based on FD and TD analysis. Included shall be a description of the fatigue capacity models (SN curves) that are available for the different mooring components. Codes and guidelines given by DNV-OS-E310, API RP 2SK and ISO 19901-7 shall be used.
- 4) Establish numerical simulation models for TD and FD analysis. Select the water depth, the mooring system and the metocean design basis reported during the project work. Use the FD design method to size a mooring system to comply with the requirements for intact mooring (safety factor = 2.2, use results from the project work!). Establish a long term environmental time series (wave, wind and ocean current description) appropriate for use in a FLS design. Perform a long term simulation in both the FD and TD and store selected line tension responses to be used in the FLS design.
- 5) Estimate the fatigue damage of selected components by using results from the FD and TD simulations. Discuss the results. The sea states contributing most to the fatigue damage shall be reported as well as the most critical mooring line components.
- 6) Examine the possibility to estimate fatigue damage by using information from the ULS design results together with a simplified method using the long term distribution of line tensions.
- 7) Conclusions and recommendations for further work.

General information

All necessary input data is assumed to be provided by Statoil.

The work scope may prove to be larger than initially anticipated. Subject to approval from the supervisor, topics may be reduced in extent.

In the thesis the candidate shall present his personal contribution to the resolution of problems within the scope of the thesis work

Theories and conclusions should be based on mathematical derivations and/or logic reasoning identifying the various steps in the deduction.

The candidate should utilise the existing possibilities for obtaining relevant literature.

Thesis format

The thesis should be organised in a rational manner to give a clear exposition of results, assessments, and conclusions. The text should be brief and to the point, with a clear language. Telegraphic language should be avoided.

The thesis shall contain the following elements: A text defining the scope, preface, list of contents, summary, main body of thesis, conclusions with recommendations for further work, list of symbols and acronyms, references and (optional) appendices. All figures, tables and equations shall be numerated.

The supervisor may require that the candidate, in an early stage of the work, presents a written plan for the completion of the work.

The original contribution of the candidate and material taken from other sources shall be clearly defined. Work from other sources shall be properly referenced using an acknowledged referencing system.

The report shall be submitted in two copies:

- Signed by the candidate
- The text defining the scope included
- In bound volume(s)
- Drawings and/or computer prints which cannot be bound should be organised in a separate folder.

Ownership

NTNU has according to the present rules the ownership of the thesis. Any use of the thesis has to be approved by NTNU (or external partner when this applies). The department has the right to use the thesis as if the work was carried out by a NTNU employee, if nothing else has been agreed in advance.

Thesis supervisor:

Prof. II Kjell Larsen (Statoil/NTNU)

Deadline: June 10, 2015

Trondheim, January, 2015

Kjell Larsen (signature):

January 2015, Kjell Larsen

Mohammad Hasan Saidee (signature):

January 2015, M. Saidee

Abstract

This master thesis deals with several problems in connection with the evaluation of fatigue damage for mooring lines. One basic problem is to find out the sea states contributing most to the fatigue loads characterized by the waves height (H_s) and the spectral peak period (T_p). This problem is investigated by designing an intact mooring system and carrying out long term simulations both in frequency domain (FD) and time domain (TD). It is found that sea states with wave heights from 6m to 10m and peak periods from 10s to 16s give higher fatigue damage.

In addition to this, comparative studies of different methods that are available to calculate mooring lines fatigue damage have been carried out both in time domain and frequency domain. It will help the mooring systems designers to decide which method to apply for a particular case. It is found that rain flow counting method based on TD analysis gives much higher fatigue damage comparing to others based on FD analysis. Simple summation approach underestimates the damage and combined narrow band approach overestimates the damage in contrast with dual narrow-band approach which is assumed to give relatively accurate result.

In this thesis especially the fatigue damage of the mooring system of ship-shaped FPSO units are assessed. For all direction of environmental loading it is observed that leeward lines experience higher fatigue than windward line. It is a special phenomenon of ship-shaped FPSO which is caused due to elliptically looped wave frequency motion of the vessel.

A simplified method is proposed here to estimate fatigue damage by using information from the ULS design results. The intention is to find a simplified way to check whether the mooring systems satisfy fatigue limit state (FLS) design criteria, especially for MODUs which are usually not designed against fatigue. It will also give an idea whether a detail fatigue analysis is needed or not.

Apart from this, relevant literature and existing mooring and station keeping systems have been reviewed.

Table of Contents

Preface.....	i
Scope of Work.....	iv
Abstract	vii
Table of Contents	ix
List of Figures	xiii
List of Tables.....	xv
Nomenclature	xvii
1 Introduction.....	1
1.1 Background for master thesis	1
2 Mooring System.....	3
2.1 Functional requirements	3
2.2 Permanent and mobile mooring system.....	3
2.3 Types of mooring system	3
2.4 Typical arrangements and components	4
3 Design of Mooring System	7
3.1 General theory	7
3.1.1 Time domain approach - theory for SIMO.....	8
3.1.2 Time domain approach - theory for RIFLEX.....	9
3.1.3 Frequency domain approach - theory for MIMOSA.....	11
3.2 Excitation forces	15
3.3 Damping	17
3.4 Stiffness	19
3.5 Environmental loads to vessel motion.....	22
3.6 Design procedure – flow chart.....	22
4 Rules and Regulation for Mooring	25
4.1 Design limit states	25
4.2 Required safety factors for ULS and ALS.....	25
4.3 FLS acceptance criteria for the Norwegian Continental Shelf (NCS).....	26
5 Fatigue Assessments	29
5.1 Frequency response method	31
5.1.1 Simple summation approach (SS).....	31

5.1.2	Combined spectrum approach (CS)	31
5.1.3	Dual narrow band approach (DNB)	32
5.2	Time domain analysis	32
5.2.1	Weibull approach	32
5.2.2	Rain-flow counting approach (RFC).....	33
5.3	Fatigue analysis procedure	34
5.4	Parameters for comparison of fatigue damage	35
6	Model Description	37
6.1	Vessel description.....	37
6.1.1	Main particulars and layout.....	37
6.1.2	Hydrodynamic properties	38
6.2	Environmental loads	39
6.3	Mooring lines properties.....	41
6.4	MIMOSA Model	42
6.5	SIMA simulation model	43
6.6	Model verification	44
6.7	Important issues during modeling (errors and solutions)	45
6.7.1	Error related to drag coefficient	46
6.7.2	Error related to modeling of leeward line of ship shaped units	46
7	Post-processing Procedure	49
8	Results and Discussions	51
8.1	Comparison between MIMOSA (FD analysis) and SIMA (TD analysis).....	51
8.2	Comparative study between fatigue calculation methods	53
8.3	Fatigue damage of windward and leeward line	54
8.4	Effect of directional probability on fatigue damage	55
8.5	Important sea states for fatigue damage	56
8.6	Simplified method for estimating fatigue damage (FLS) from the ULS results	58
9	Conclusion	61
9.1	Conclusion from results and discussion	61
9.2	Recommendation for future work.....	62
10	Bibliography.....	63
	APPENDIX A	65
	APPENDIX B	66

APPENDIX C	67
MIMOSA mooring file	67
MIMOSA macro file for long term simulation	69
APPENDIX D	74
All plots for vessel hydrodynamic properties	74
APPENDIX E.....	77
APPENDIX F.....	78
Matlab script for getting vessel data from MIMOSA vessel file	78
Matlad script for plotting	80

List of Figures

Figure 1-1 Turret-moored production ship - Norne FPSO (Larsen K. , 2014)	1
Figure 2-1 Basics types of mooring system (Larsen K. , 2014).....	4
Figure 2-2 Typical arrangement of mooring system (Larsen K. , 2014)	5
Figure 2-3 Main mooring line components.....	5
Figure 3-1 Directions of vessel motion and environmental loads for mooring system	7
Figure 3-2 Calculation of vessel offset in MIMOSA (Larsen K. , 2014)	11
Figure 3-3 Dynamic load factor as function of the frequency ratio for given values of damping ratio (Larsen C. M., 2012).....	18
Figure 3-4 Phase angle between load and response as function of the frequency ratio for given values of damping ratio (Larsen C. M., 2012)	18
Figure 3-5 Elastic stiffness of mooring line (Larsen K. , 2014).....	20
Figure 3-6 Geometrical stiffness of mooring line (Larsen K. , 2014).....	20
Figure 3-7 Horizontal stiffness from one mooring line (Larsen K. , 2014).....	21
Figure 3-8 Iteration process for mooring system analysis	23
Figure 4-1 Characteristic Tension from probability distribution of tension	26
Figure 5-1 The Miner summation procedure; (a) stress range (b) S-N curve (Berge, 2006)...	29
Figure 5-2 Design S-N curves for Mooring lines (DNV, 2013)	30
Figure 5-3 Long term distribution of stress range (Almar-Næss, 1985).....	33
Figure 5-4 Rain-flow cycle counting procedure (Berge, 2006)	34
Figure 6-1 Åsgard A FPSO	37
Figure 6-2 Current force coefficient (Direction - going towards).....	38
Figure 6-3 Wind force coefficient (Direction - coming from)	38
Figure 6-4 RAOs for surge, heave and pitch.....	39
Figure 6-5 Heidrun 1, 10, 100 and 10000-year extreme contour lines in H_s - T_p plane (Statoil, 2004).....	40
Figure 6-6 line characteristics curve indicating horizontal tension vs. distance to anchor.....	42
Figure 6-7 Definition of directions for force coefficients and RAOs in MIMOSA file	42
Figure 6-8 Old form of LTS input of environmental file (MIMOSA, 2012).....	43
Figure 6-9 Horizontal (right) and vertical (left) projections of the mooring lines.....	43
Figure 6-10 SIMA simulation model	44
Figure 6-11 Comparison of restoring force in SIMA and MIMOSA model	45
Figure 6-12 Time history of axial force of mooring line without (right) and with (left) longitudinal drag coefficient	46
Figure 6-13 Compression pulsations (red regions) in leeward mooring	47
Figure 6-14 Modeling error - excessive axial force on mooring line.....	47
Figure 6-15 Time series of tension process for sea state $H_s = 16\text{m}$ and $T_p = 18.2\text{s}$	48
Figure 7-1 SIMA post-processing tool for fatigue damage calculation	49
Figure 8-1 Offset for wave frequency tension calculation in MIMOSA	52
Figure 8-2 Comparative study of different fatigue analysis method.....	53
Figure 8-3 Dynamic effect on leeward and windward mooring line	55
Figure 8-4 Fatigue damage for all lines in all direction using DNB approach	56
Figure 8-5 Scatter diagram probability of sea states	57

Figure 8-6 Fatigue damage calculated by MIMOSA (left) and SIMA (right) for line 1 57
Figure 8-7 Fatigue damage calculated by MIMOSA (left) and SIMA (right) for line 7 58
Figure 8-8 Approximate shape of long term stress distribution..... 60

List of Tables

Table 2-1 Comparison of properties for mooring line materials (Larsen K. , 2014) 6

Table 3-1 Contribution of environmental loads to vessel motion 22

Table 4-1 Safety factors for permanent oil storage or production units (Larsen K. , 2014) 26

Table 4-2 Safety factors for mobile drilling units (Larsen K. , 2014)..... 26

Table 5-1 S-N fatigue curve parameters (DNV, 2013) 31

Table 6-1 Main particulars of Åsgard A FPSO 37

Table 6-2 Modified scatter diagram of sea states 40

Table 6-3 Direction probability of environmental loads (Statoil, 2004) 40

Table 6-4 Properties of mooring lines 41

Table 6-5 Equilibrium position of vessel from MIMOSA and SIMA 45

Table 6-6 Environmental loads in X-direction (surge) from MIMOSA and SIMA 45

Table 8-1 Standard deviation of tension process 51

Table 8-2 Tension values on top of mooring line calculated by MIMOSA and SIMA 52

Table 8-3 Fatigue damage of windward and leeward line for all direction 54

Table 8-4 Results from ULS design condition ($H_s = 16\text{m}$ and $T_p = 18.2\text{s}$) 59

Table 8-5 Approximate values of Weibull parameter, h 60

Nomenclature

General rules:

- Parameters used in equations are explained after the equations have been used
- Abbreviations are given after the first use of the terms

Roman Letters:

a_D – S-N curve parameter
 C_{wi} – Wind force coefficient
 C_{cu} – Current force coefficient
 C_D – Drag coefficient
D or d – Fatigue damage
 d_c – Characteristic fatigue damage
 h – Weibull parameter
 $H(\omega)$ – Transfer function
 H_s – Significant wave height
 m – S-N curve parameter
 n_0 – Number of stress cycle
 R_C – Characteristic strength
 sf – Safety factor
 x or X – Offset in X-direction
 T_p – Peak period
 T – Tension
 T_z – Mean up-crossing period

Greek Letters:

ω – Frequency in Hertz
 σ – Standard deviation
 ν – Mean up-crossing rate in Hertz
 δ_W – Bandwidth parameter
 γ_F – The single safety factor for the fatigue limit state

Abbreviations:

ALS – Accidental limit estate
CS - Combined spectrum
DNB - Dual narrow-band
FLS – Fatigue limit state
FPSO – Floating Production, Storage and Offloading
FD – Frequency domain
LF – Low frequency
LTS – Long term simulation
MODU - Mobile Drilling Units
MPM – Most probable largest
NCS - Norwegian Continental Shelf
RAO – Response amplitude operator
RFC - Rain flow counting

SS - Simple summation
TD – Time domain
ULS – Ultimate limit state
WF – Wave Frequency

1 Introduction

In the past decades, mooring failures have been occurring at an unacceptable high rate. Some of them were multiple line damages, leading to vessel drifting. Much effort has been done in order to investigate the events in order to find the main reasons. The investigations show a variety of direct causes covering both inaccurate design, bad quality on mooring line components and lack of personnel competence related to operation of the system.

The mooring of FPSOs (Figure 1-1) and permanent floaters tend to be more of a complex nature as the industry is moving into new frontiers (ultra-deep water down to 3000m depth and into arctic areas) and the new units are becoming larger and many units are at the end of their lifetime. Fatigue analysis of mooring lines is required for these units and lots of fatigue analyses have already been done on production facilities and flotels before.



Figure 1-1 Turret-moored production ship - Norne FPSO (Larsen K. , 2014)

1.1 Background for master thesis

The work in this thesis is focused on the improvement of the design of FPSO mooring system especially against the fatigue damage. It is based on the work performed during the project work carried out autumn 2014, but the focus and content of this MSc is related to the fatigue design of mooring components according to the Fatigue Limit State (FLS) criteria.

The main objective of the thesis is to estimate the fatigue damage of selected components by using results from the FD and TD simulations and also to find out the sea states contributing most to the fatigue damage.

According to (DNV, 2013) the fatigue damage on mooring lines can be calculated using different methods e.g. simple summation (SS), combined spectrum (CS), Dual narrow-band (DNB) and rain-flow counting method. So, it is of interest to know the effect of using different methods on the calculated fatigue damage. A chapter in this thesis will deal with this issue.

The MIMOSA program will be used for frequency domain analysis and the SIMA program will be used for fully coupled approach in time domain. As two different software packages are used the models in both software's need to be equivalent. So, some checks have been carried out and the verification of the model is included in a separate chapter.

In addition to these, an analysis will be performed for the chosen sea state which gives highest fatigue damage to check in detail which parameters are important and responsible for the differences in results.

A study is also conducted to examine the possibility to estimate fatigue damage by using information from the ULS design results together with a simplified method using the long term distribution of line tensions.

2 Mooring System

2.1 Functional requirements

The mooring systems normally have 12-16 mooring lines consisting of heavy chain, steel wire ropes and synthetic materials (polyester) connected to a seabed anchor. The purpose of the mooring system is to keep the floating vessel safely at a required position and to limit the horizontal offset of the floating structure to an acceptable limit so that:

- Integrity of risers and umbilicals is maintained
- Safe distance to other structures is maintained
- Control the mean offset and low-frequency motions
- Absorb the wave-frequency motions

The station-keeping system is also very important for marine safety. It is possible to avoid collision accident by having a reliable station-keeping system.

2.2 Permanent and mobile mooring system

In a mobile mooring system anchoring at a specific location is done for a period less than 5 years e.g. mooring of Mobile Drilling Units whereas for a permanent mooring system mooring of a unit remains at the same location for more than 5 years e.g. mooring of FPSOs. Mobile Drilling Units (MODUs) have different anchor requirements than permanently moored systems. The permanent mooring is designed to meet the strength and fatigue requirements of a project and the anchors are usually not retrieved. Anchors and mooring lines for temporary moorings need to be more robust to withstand repetitious handling, installation and retrieval. Usually they are not designed for fatigue limit state rather they are checked by class society every five years before installing in a new location.

2.3 Types of mooring system

Types of mooring system can be divided into two categories known as turret mooring and spread mooring system. It is important to recognize that turret mooring and spread mooring have different performance characteristics, both in terms of vessel motion which can affect topside operations and offloading systems.

Turret mooring:

Turret mooring system is weather vaning type meaning the vessel can rotate around the turret axis depending on the weather conditions. Ship-shaped FPSO usually requires turret mooring in order to minimize environmental loads. Turrets can be of three types (Figure 2-1):

- I. Internal turrets
- II. Disconnectable internal turrets
- III. External turrets

The internal moored system is integrated into the forward end of the vessel, where there is a large roller bearing which is either located in the moon pool or at the deck level. An external

moored system is situated outside the vessel hull and can be located close to the bow or stern of the vessel. Disconnectable internal turrets are similar to internal turrets except it can be disconnected in case of harsh weather condition. Vessel can move to a safer place and come back again when the environmental condition is convenient for operation leading no damage to the vessel, mooring lines or risers due to bad weathers.

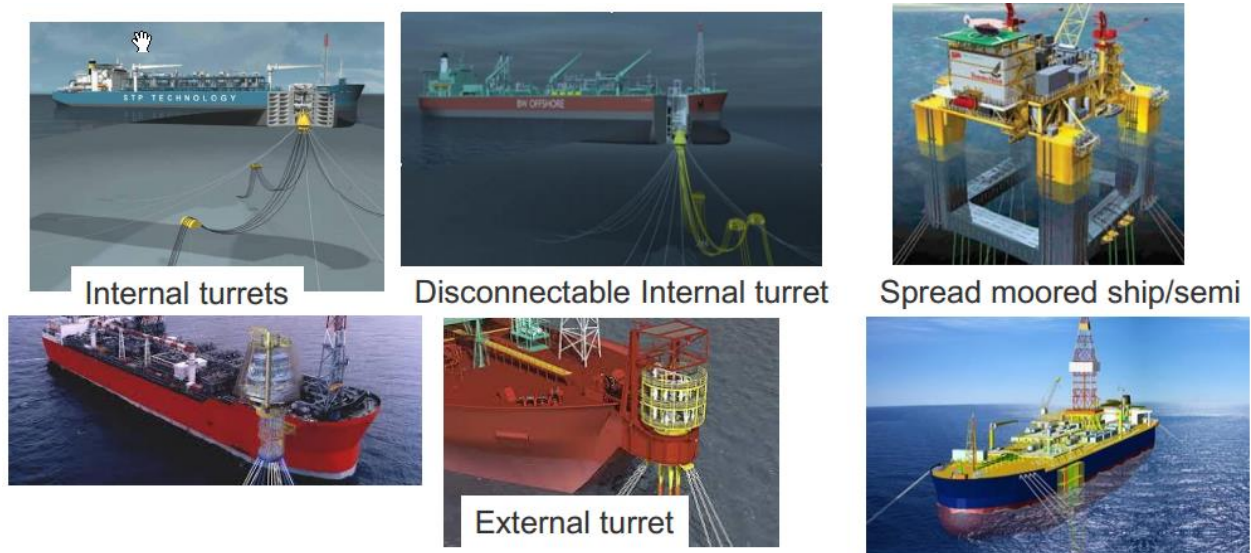


Figure 2-1 Basics types of mooring system (Larsen K. , 2014)

Spread mooring:

Spread moored system as shown in Figure 2-1 has fixed orientation and multi point mooring system that contains multiple mooring lines to moor the vessel. They are usually used where the weather condition is not that severe. In this system the vessel has a fixed heading and the bow is typically positioned against the dominant environmental direction especially the direction from which the largest waves are coming from. This type of mooring is considered to be less costly than previous one. But as the turret mooring system is a single point mooring it aligns itself to the environment and provides a means for offloading from the stern which is more convenient whereas fixed orientation of the spread moored system and changing environmental conditions make offloading operations more difficult.

2.4 Typical arrangements and components

Mooring system arrangements:

There are three types of arrangement for mooring system known as taut mooring, catenary mooring and catenary mooring with buoyancy elements. Components that are used for these arrangements are given below.

- Taut mooring comprises of chain- synthetic fiber ropes/polyester-chain.
- Catenary mooring comprises of chain-steel rope-chain
- Catenary mooring with buoyancy elements comprises of chain-steel wire rope-buoy-steel wire rope –chain.

When oil and gas extraction was conducted in shallow to deep water, catenary systems were more popular but with the introduction of production in deep to ultra-deep water the weight of the mooring lines become a limiting factor. To overcome this problem, new solutions were developed named as taut leg mooring system. The main difference between these systems are that where in a catenary system mooring lines arrives at the seabed horizontally, the taut mooring arrives at an angle (Vryh of Anchors BV, 2010). This means that taut mooring anchor point is capable of resisting both horizontal and vertical forces, while catenary mooring anchor point subjected to horizontal forces only. Another important difference is that the restoring force in catenary mooring is generated by the weight of the components whereas the restoring force of a taut mooring comes from the elasticity of the mooring line.

In Figure 2-2 different arrangements for mooring system is shown.

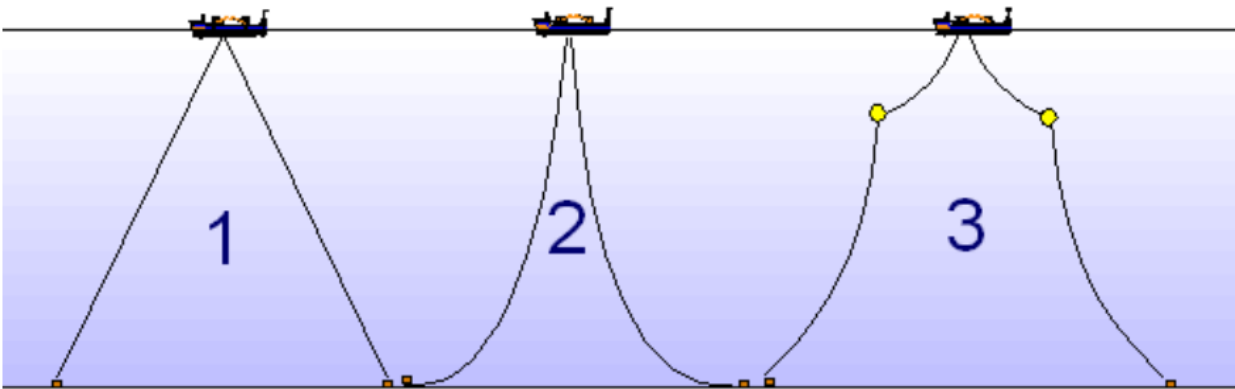


Figure 2-2 Typical arrangement of mooring system (Larsen K. , 2014)

(1-taut mooring, 2-catenary mooring and 3-catenary mooring with buoyancy elements)

Mooring line components:

Mooring lines can have several components e.g. anchor, chain, connecting links, steel wire ropes, synthetic fiber ropes, buoys, clump weights etc. Some mooring components are shown in Figure 2-3.

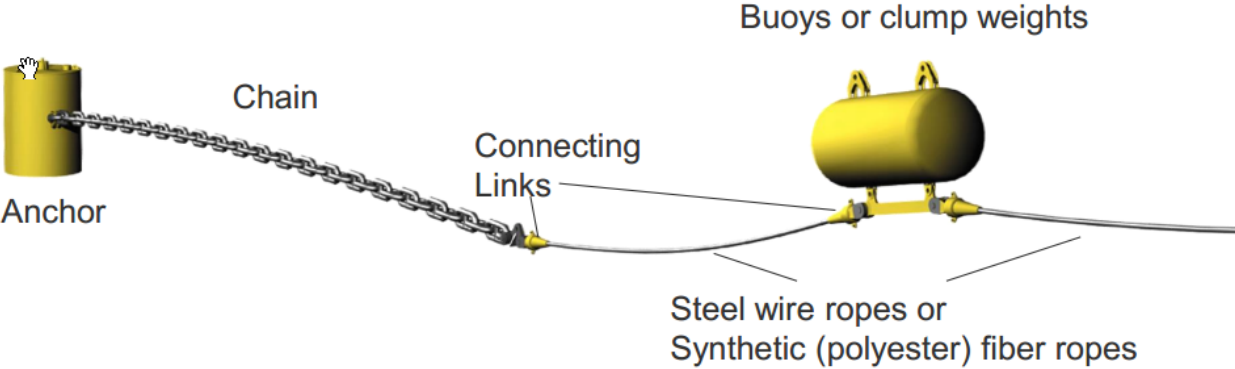


Figure 2-3 Main mooring line components

Materials for a mooring line can be of three types namely chain, steel wire rope and synthetic fiber rope. Properties of these materials are given below.

Chain: Chain can be studless or studlink. Studlink chains are used when those are reset numerous time during their life time, for instance mooring line of semi-submersibles and studless are used for permanent mooring e.g. mooring of FPSOs. Usually they have heavy weight, high stiffness (Table 2-1) and good abrasion characteristics. But they are likely to experience more fatigue damage in comparison with others.

In the following table properties of three different mooring line materials for a 1000 tonnes breaking strength rope are given.

Table 2-1 Comparison of properties for mooring line materials (Larsen K. , 2014)

Material	Diameter (mm)	Weight in air (kg/m)	Weight in water (kg/m)	Typical Axial Stiffness* 10^{-5} (kN)
Stud R4 chain	102	230	200	7
Spiral strand steel	108	57	48	9
Polyester	175	23	5.9	1.0 – 4.5

Steel wire rope: Usually comprises of spiral strands and uncovered or covered with plastic sheet. Wire ropes are lighter than chains as given in the above table. Generally accepted as having good fatigue properties, the ropes themselves may not be a concern. However, for any connecting components, typically chains and shackles, experience from traditional shallow water moorings readily shows fatigue capacity to be marginal or even the limiting factor in design (Vryh of Anchors BV, 2010).

Synthetic fiber rope: Usually made of polyester but other high tech fibers also exist. Fiber ropes have less weight but high elasticity. Predictions of the long term (fatigue) characteristics (FLS) are less obvious and usually require more time consuming and complex calculations. Some of the advantages of using polyester mooring lines are as follows:

- Reduced floater offset due to taut leg configuration which is comparatively simpler solution for riser design
- Reduced weight which contributes for increased pay load on floaters
- Suitable if cross-over flow lines or pipelines are present nearby
- As it requires smaller foot print the line length is reduced
- And overall cost is expected to be reduced for deep water mooring system

3 Design of Mooring System

3.1 General theory

In this chapter the theory behind solving the equation of motion will be discussed. For simplicity only the horizontal motion (surge) in x-direction is considered here as shown in the figure below.

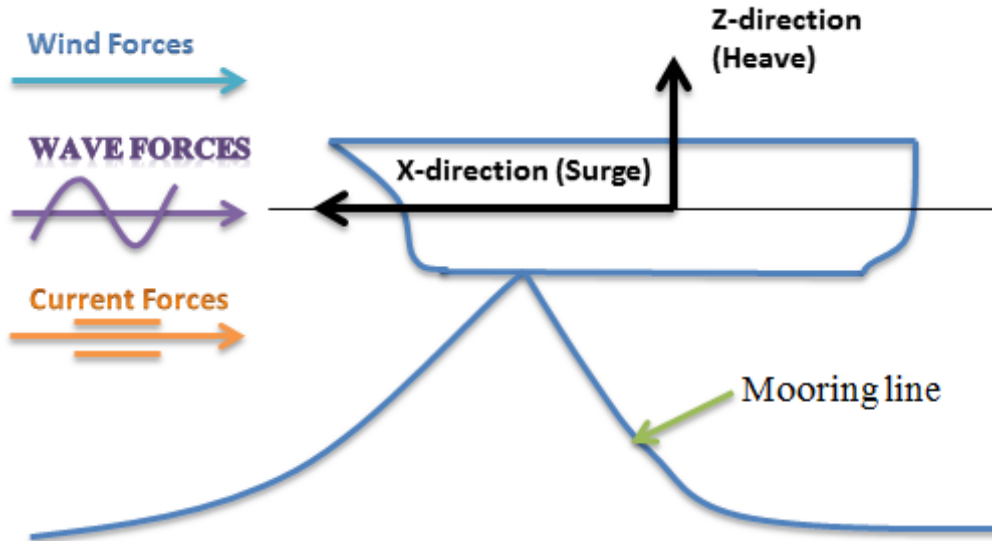


Figure 3-1 Directions of vessel motion and environmental loads for mooring system

The equation of motion for sinusoidal motion can be written as:

$$M\ddot{x} + C\dot{x} + D_l\dot{x} + D_q\dot{x}|\dot{x}| + K(x)x = Q(t, x, \dot{x}) \quad [3-1]$$

and,

$$\begin{aligned} M &= m + A(\omega) \\ A(\omega) &= A_\infty + a(\omega) \\ A_\infty &= A(\omega = \infty) \\ C(\omega) &= C_\infty + c(\omega) \\ C_\infty &= C(\omega = \infty) \equiv \mathbf{0} \end{aligned} \quad [3-2]$$

Where:

M = Frequency-dependent mass matrix

m = body mass matrix

A = Frequency-dependent added mass

C = Frequency-dependent potential damping matrix

D_l = Linear damping matrix

D_q = Quadratic damping matrix

K = Hydrostatic stiffness matrix

x = Position vector

Q = Excitation force vector

3.1.1 Time domain approach - theory for SIMO

The content in this chapter is taken from SIMO theory manual (SIMO, 2012).

Two different solution methods are available for solving this equation; one is by using convolution integral and another one is separation method. Using the convolution integral the equation of motion can be written as:

$$(\mathbf{M} + \mathbf{A}_\infty)\ddot{\mathbf{x}} + \mathbf{D}_l\dot{\mathbf{x}} + \mathbf{D}_q\dot{\mathbf{x}}|\dot{\mathbf{x}}| + \mathbf{K}(x)\mathbf{x} + \int_0^t h(t-\tau)\dot{\mathbf{x}}(\tau)d\tau = \mathbf{Q}(t, \mathbf{x}, \dot{\mathbf{x}}) \quad [3-3]$$

Total derivation of the above equation can be found in section 4.1.1 (SIMO, 2012) and $h(\tau)$, the retardation function is computed by a transformation of frequency-dependent added mass and damping:

$$h(\tau) = \frac{1}{2\pi} \int_{-\infty}^{\infty} c(\omega) + i\omega a(\omega) e^{i\omega\tau} d\omega = \frac{1}{2\pi} \int_{-\infty}^{\infty} \mathbf{H}(\omega) e^{i\omega\tau} d\omega \quad [3-4]$$

Or similarly:

$$\mathbf{H}(\omega) = \int_{-\infty}^{\infty} h(\tau) e^{i\omega\tau} d\tau = c(\omega) + i\omega a(\omega) \quad [3-5]$$

Using the fact that $c(\omega) = c(-\omega)$ and $a(\omega) = a(-\omega)$ gives:

$$h(\tau) = \frac{1}{\pi} \int_0^{\infty} c(\omega) \cos \omega\tau - \omega a(\omega) \sin \omega\tau d\omega \quad [3-6]$$

From casualty, $h(\tau) = 0$ for $\tau < 0$; the process can not have any memory effect of the future. This means that the two parts in the integral, mathematically:

$$h(\tau) = \frac{2}{\pi} \int_0^{\infty} c(\omega) \cos \omega\tau d\omega = -\frac{2}{\pi} \int_0^{\infty} \omega a(\omega) \sin \omega\tau d\omega; \text{ for } \tau > 0 \quad [3-7]$$

This means that the frequency-dependent mass and damping can be found from the retardation function:

$$a(\omega) = -\frac{1}{\omega} \int_0^{\infty} h(\tau) \sin \omega\tau d\tau \quad [3-8]$$

$$c(\omega) = -\frac{1}{\omega} \int_0^{\infty} h(\tau) \cos \omega \tau \, d\tau \quad [3-9]$$

Either frequency-dependent added-mass or frequency-dependent damping and one value of the added mass are required to calculate the retardation function and damping expression is preferred due to numeric.

The motions can be separated in a high-frequency part and low-frequency part. As an alternative to solve whole differential equation in time domain, the high-frequency part (also known as wave-frequency) can be solved in frequency domain but the motion needs to be linear response to waves by making quadrating damping (\mathbf{D}_q) zero and stiffness \mathbf{K} constant.

The excitation force is separated in a wave frequency part, \mathbf{Q}_{WF} (high-frequency part) and a low-frequency part, \mathbf{Q}_{LF} using the following equation.

$$\mathbf{Q}(t, \mathbf{x}, \dot{\mathbf{x}}) = \mathbf{Q}_{WF} + \mathbf{Q}_{LF} \quad [3-10]$$

And the position vector can be separated using high frequency offset, \mathbf{x}_{WF} and low-frequency offset, \mathbf{x}_{LF} part:

$$\mathbf{x} = \mathbf{x}_{WF} + \mathbf{x}_{LF} \quad [3-11]$$

The equation for solving the high-frequency motion in frequency domain is given below:

$$\mathbf{M} + \mathbf{A}(\omega) \ddot{\mathbf{x}}_{WF} + \mathbf{D}_I \dot{\mathbf{x}}_{WF} + \mathbf{C}(\omega) \dot{\mathbf{x}}_{WF} + \mathbf{K} \mathbf{x}_{WF} = \mathbf{Q}(t, \mathbf{x}, \dot{\mathbf{x}}) \quad [3-12]$$

In order to solve the above equation in frequency domain we can use:

$$\mathbf{X}_{WF}(\omega) = \left(-\omega^2 (\mathbf{m} + \mathbf{A}(\omega)) + i\omega \mathbf{D}_I + \mathbf{C}(\omega) + \mathbf{K} \right)^{-1} \mathbf{H}_1(\omega) \zeta(\omega) \quad [3-13]$$

Where \mathbf{H}_1 is the 1st order transfer function between excitation force and wave elevation and \mathbf{H}_{WF} is the 1st order transfer function between motion and wave elevation.

The two-frequency motions can be solved using the dynamic equilibrium equation:

$$\mathbf{m} + \mathbf{A}(\omega = \mathbf{0}) \ddot{\mathbf{x}}_{LF} + \mathbf{D}_I \dot{\mathbf{x}}_{LF} + \mathbf{D}_q \dot{\mathbf{x}}_{LF} |\dot{\mathbf{x}}_{LF}| + \mathbf{K} \mathbf{x}_{LF} = \mathbf{Q}_{LF} \quad [3-14]$$

3.1.2 Time domain approach - theory for RIFLEX

The content in this chapter is taken from RIFLEX theory manual (RIFLEX, 2013).

The mooring lines are discretized into numbers of small elements and the dynamic equilibrium of a spatial discretized element that RIFLEX solve for TD analysis is given below.

$$R^I(r, \ddot{r}, t) + R^D(r, \dot{r}, t) + R^S(r, t) = R^E(r, \dot{r}, t) \quad [3-15]$$

Where,

R^I – Inertia force vector

R^D – Damping force vector

R^S – Internal structural reaction force vector

R^E – External force vector

r, \dot{r}, \ddot{r} – Structural displacement, velocity and acceleration vector

The inertia force vector and damping load vector are obtained by:

$$R^I(r, \ddot{r}, t) = \mathbf{M}(r)\ddot{r} \quad [3-16]$$

$$R^D(r, \dot{r}, t) = \mathbf{C}(r)\dot{r} \quad [3-17]$$

Here \mathbf{M} is the system mass matrix and \mathbf{C} is the system damping matrix.

In a coupled analysis the large volume body e.g. FPSO is introduced as a nodal component in the FEM model. The body forces are computed for each time step and included in the external load vector, R^E .

This is a nonlinear system of differential equations and step by step numerical time integration is used to solve the above dynamic equilibrium equation in order to get the tension and offset of the mooring line. The incremental form of above equation is obtained by considering dynamic equilibrium at two configurations for a short time interval, Δt :

$$(R^I_{t+\Delta t} - R^I_t) + (R^D_{t+\Delta t} - R^D_t) + (R^S_{t+\Delta t} - R^S_t) = (R^E_{t+\Delta t} - R^E_t) \quad [3-18]$$

This equation states that increment in external loading is balanced by increments in inertia, damping and structural reaction force over the time interval, Δt .

Newton-Raphson type equilibrium iteration can be used at each time step which allows for all nonlinearities. But it is rather time consuming due to repeated assembly of system matrices (mass, damping and stiffness) and triangularisation during each time step.

Linearized time domain analysis can be used to reduce the computation time. In this approach step by step numerical integration of the dynamic equation is done by linearization of mass, damping and stiffness matrices at static equilibrium position.

3.1.3 Frequency domain approach - theory for MIMOSA

The content in this chapter is taken from MIMOSA user's documentation (MIMOSA, 2012).

In case of frequency domain both the equation [3-10] and [3-11] are used to separate WF and LF part and both of them are solved in frequency domain.

When the frequency domain approach is used for simulation of vessel dynamics, the maximum offset is defined as the mean offset plus maximum displacement due to combined wave frequency and low frequency vessel motion as shown in Figure 3-2. Maximum offset can be determined by the following procedure (MIMOSA, 2012).

Let,

X_{mean} = Mean vessel offset

X_{max} = Maximum vessel offset

X_{WFmax} = Maximum wave frequency motion

X_{WFsig} = Significant wave frequency motion

X_{LFmax} = Maximum low frequency motion

X_{LFsig} = Significant low frequency motion

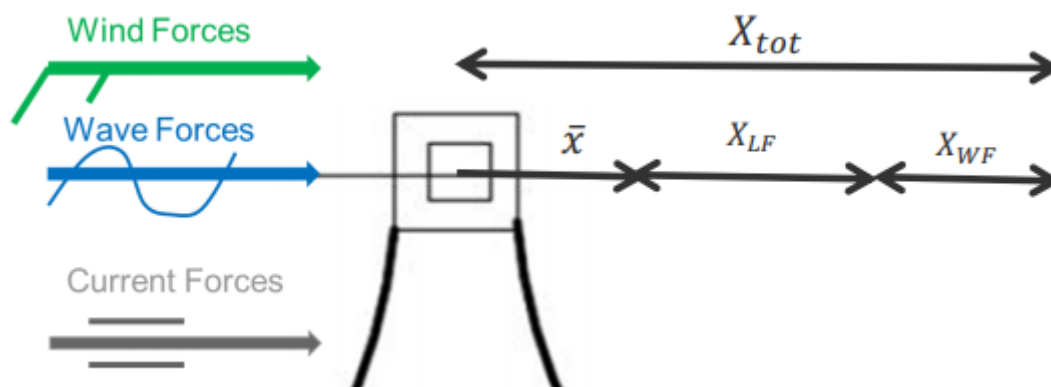


Figure 3-2 Calculation of vessel offset in MIMOSA (Larsen K. , 2014)

The maximum offset is the larger one between the values obtained by the following two equations. A visual representation is given in Figure 3-2.

$$X_{max} = X_{mean} + X_{LFmax} + X_{WFsig} \quad [3-19]$$

$$X_{max} = X_{mean} + X_{WFmax} + X_{LFsig} \quad [3-20]$$

Mean offset (static equilibrium):

The mean position of the vessel for a particular environmental condition is computed by finding the position of it where equilibrium is established between the mean environmental loads (wave, wind and current) and the restoring forces from the positioning system.

$$\text{Mean Load, } \bar{F} = \bar{F}_{wa} + \bar{F}_{wi} + \bar{F}_{cu} \quad [3-21]$$

$$\text{Static equilibrium, } K(x).x = \bar{F} \quad [3-22]$$

Here, x is the mean offset defined by X_{mean} .

Mimosa computes the equilibrium by a numerical procedure that solves the equation (MIMOSA, 2012),

$$F^{mo}(x) + F^{hs}(x) + F^{th}(x) + F^{cu}(x) + F^{wi}(x) + F^{wa}(x) + F^{fi}(x) = 0 \quad [3-23]$$

Here, $F^{mo}(x)$ – Mooring Force

$F^{hs}(x)$ – Hydrostatic force

$F^{th}(x)$ – Thruster force

$F^{cu}(x)$ – Current force

$F^{wi}(x)$ – Wind force

$F^{wa}(x)$ – Wave force

$F^{fi}(x)$ – Fixed force

The solution to equation [3-23] is the equilibrium position.

Wave frequency motion offset:

Wave frequency motion response is computed without regard to the mooring system. This is due to the fact that the mooring system will usually not modify vessel's transfer function noticeably. The first order wave frequency motion is computed using the wave spectrum and the six linear transfer functions from waves to vessel motion. If we denote $S_{\zeta}^{WF}(\omega, \beta)$ as the spectral density for wave propagation and β as the direction relative to vessel, then for each motion the WF response spectrum will be,

$$S_{x_i}^{WF}(\omega) = \int_0^{2\pi} |H_i^{WF}(\omega, \beta)|^2 S_{\zeta}^{WF}(\omega) d\omega \quad [3-24]$$

Here, $H_i^{WF}(\omega, \beta)$ is the transfer function or RAOs for different vessel motions

The standard deviation of the response are then computed using equation [3-25].

$$\sigma_{X-WF} = \sqrt{\int_0^{\infty} S_{x_i}^{WF}(\omega) d\omega} \quad [3-25]$$

In order to calculate the significant and largest motion it is assumed that the response is a narrow banded Gaussian process, so that the peaks are Rayleigh distributed. The significant value is the mean value of the one-third highest peaks of motion from Rayleigh distribution and it is almost exactly twice the value of the standard deviation. On this basis, the significant and largest value is defined as,

$$X_{WFsig} = 2\sigma_{X-WF} \quad [3-26]$$

$$X_{WFmax} = \sigma_{X-WF} \sqrt{2 \ln N_{WF}} \quad [3-27]$$

Where, N_{WF} is the number of wave-frequency platform oscillations during the duration of the environmental state that is normally 3 hours.

Low frequency motion offset:

The LF motion estimation is based on a linearization of the restoring forces (stiffness) and damping and on linearized LF excitation forces from wind and waves (force spectrum). The linearized system must be dynamically stable. So, for turret moored ships it should be checked.

According to (MIMOSA, 2012) the slowly varying horizontal motion is computed by solving the linear equation [3-28].

$$M\ddot{x}^{LF} + C\dot{x}^{LF} + Kx^{LF} = F^{LF} \quad [3-28]$$

Here, x^{LF} and F^{LF} are the LF position response vector and LF load vector respectively.

The matrix transfer function is given by,

$$H^{LF}(\omega) = [-\omega^2 M + j\omega C + K]^{-1}, \quad j = \sqrt{-1} \quad [3-29]$$

Similarly as the wave frequency, for low frequency motion,

$$X_{LFsig} = 2\sigma_{X-LF} \quad [3-30]$$

$$X_{LFmax} = \sigma_{X-LF} \sqrt{2 \ln N_{LF}} \quad [3-31]$$

Where, N_{LF} is the number of low-frequency platform oscillations during the duration of the environmental state that is normally 3 hours.

Calculation of mooring line tension:

When quasi-static analysis is applied the tension at the top end is assumed to dependent only on the top end horizontal distance and vertical distance from the anchor as in equation [3-32].

$$T = T(r) \quad [3-32]$$

Where, $r = (x, z)$ is the distance vector from the anchor to the upper end.

According to (DNV, 2013) we can calculate the quasi-static tension for the upper terminal point $T_{QS}(X_{max})$, using position X_{max} and for the mean position as $T_{mean}(X_{mean})$. Then the dynamic tension can be found using the following equation.

$$T_{dyn} = T_{QS}(X_{max}) - T_{mean}(X_{mean}) \quad [3-33]$$

In case of dynamic mooring analysis, standard deviation of tension is used assuming that the response is narrow banded Gaussian process, so that the peaks are Rayleigh distributed. The maximum wave frequency tension is the defined by:

$$T_{WFmax} = \sigma_{T-WF} [X_{max} - X_{WFmax}] \sqrt{2 \ln N_{WF}} \quad [3-34]$$

And the dynamic tension T_{dyn} is defined by:

$$T_{dyn} = T_{QS}[X_{max} - X_{WFmax}] - T_{mean}(X_{mean}) + T_{WFmax} \quad [3-35]$$

Here $T_{QS}[X_{max} - X_{WFmax}]$ is the quasi-static tension calculated at $(X_{max} - X_{WFmax})$ position.

3.2 Excitation forces

The term in the right hand side of equation [3-1] is excitation forces related to mooring analysis are Environmental loads i.e. wave, wind and current forces. If the system is thruster assisted it will have additional thruster force. All these can be expressed by the following equations (Larsen K. , 2014).

$$\mathbf{Q}(t, x, \dot{x}) = q_{wi} + q_{cu} + q_{wa} + q_{thr} \quad [3-36]$$

Here, $\mathbf{Q}(t, x, \dot{x})$ = total excitation force,

q_{wi} =Wind forces,

q_{cu} =Current forces,

q_{wa} = Wave forces, and

q_{thr} = Thruster forces

Wind forces (q_{wi}) : Wind forces are characterized by Mean value due to mean wind velocity and Low-frequency (LF) forces excited by wind gusting. Wind gusts have significant energy at surge, sway, and yaw natural oscillation periods. Dynamic wind will excite LF motions of moored floating structures. Wind forces can be found by using the following equations.

$$\text{Wind forces, } q_{wi}(t) = \frac{1}{2} \cdot \rho_{air} \cdot C_D \cdot A \cdot (U(t) - \dot{r})^2 \quad [3-37]$$

Where, $U(t) = \bar{U} + u(t)$ and \bar{U} and $u(t)$ are mean velocity and dynamic wind gust respectively.

ρ_{air} = density of air,

C_D = Drag coefficient,

$U(t)$ = Wind velocity with respect to time,

And \dot{r} = floater velocity.

So, if we expand the above equation we get,

$$q_{wi}(t) \approx \frac{1}{2} \cdot \rho_{air} \cdot C_D \cdot A \cdot (\bar{U})^2 + \rho_{air} \cdot C_D \cdot A \cdot \bar{U} \cdot u(t) - \rho_{air} \cdot C_D \cdot A \cdot \bar{U} \cdot \dot{r} \quad [3-38]$$

Here, $u(t)^2$, $2 \cdot u(t) \cdot \dot{r}$ and \dot{r}^2 terms are neglected as they will yield very low value.

The three terms in above equation give constant force, LF excitation force and LF damping force respectively. For each floating vessel wind force coefficient must be established by the following equation.

$$C_{wi} = \frac{1}{2} \cdot \rho_{air} \cdot C_D \cdot A \quad [3-39]$$

Current forces ($q_{cu}(t)$): Current forces are characterized by Mean value due to mean current velocity, but current turbulence is neglected. Current velocity is assumed constant for the time period of interest. For motion response floaters, it is the current velocity at the surface that is of primary interest. Current forces can be found using the following equation.

$$\text{Current forces, } q_{cu}(t) = \frac{1}{2} \rho_{water} C_D (\bar{V} - \dot{r}) |(\bar{V} - \dot{r})| \quad [3-40]$$

Where, \bar{V} is the current velocity, \dot{r} is the floater velocity and ρ_{water} is the density of water.

If $\bar{V} > \dot{r}$ we can write:

$$q_{cu}(t) = \frac{1}{2} \rho_{water} C_D (\bar{V} - \dot{r})^2 \quad [3-41]$$

By expand the above equation we get,

$$q_{cu}(t) \approx \frac{1}{2} \cdot \rho_{water} \cdot C_D \cdot A \cdot (\bar{V})^2 + \rho_{water} \cdot C_D \cdot A \cdot \bar{V} \cdot \dot{r} \quad [3-42]$$

Here, the term containing \dot{r}^2 is neglected as it will yield very low value

The two terms in above equation give constant force and LF damping force respectively. For each floating vessel current force coefficient must be established by the following equation.

$$C_{cu} = \frac{1}{2} \cdot \rho_{water} \cdot C_D \cdot A \quad [3-43]$$

Wave forces (q_{wa}): Wave forces are characterized by the following properties.

- 1st order forces proportional with wave amplitude, is described by force transfer functions.
- mean value due to 2nd order wave loads
- Low-frequency (LF) forces excited by 2nd order wave loads.

1st order motion due to wave, wave drift excitation and LF excitation can be found using the equations [3-44], [3-45] and [3-46].

$$S_{heave,top}(\omega) = |H_{top}(\omega)|^2 \cdot S_{wave}(\omega) \quad [3-44]$$

Where, $S_{heave,top}(\omega)$ and $S_{wave}(\omega)$ are spectrum of heave motion and wave respectively and $H_{top}(\omega)$ is the transfer function to get heave motion spectrum from wave spectrum.

$$\text{Wave forces, } q_{wa} = C_{wa}\eta^2 \quad [3-45]$$

Where, q_{wa} is the mean wave drift force, C_{wa} is wave drift force coefficient, and η is the wave amplitude.

$$S_{wa}(\mu) = 8 \cdot \int_0^\infty C_{wa}(\omega + \frac{\mu}{2}) \cdot C_{wa}(\omega + \frac{\mu}{2}) \cdot S_\eta(\omega) \cdot S_\eta(\omega + \mu) d\omega \quad [3-46]$$

Where, $S_{wa}(\mu)$ is load spectrum for frequency, μ and $S_\eta(\omega)$ is wave spectrum.

3.3 Damping

It is very important to understand the damping of a single degree of freedom system given in [3-1]. For that system DLF can be found using the following equation (Larsen C. M., 2012). DLF is the dynamic load factor and it states the ration between the dynamic and static response for the relevant load.

$$DLF = \left| \frac{x_{maks}}{x_{static}} \right| = \frac{1}{[(1 - \beta^2)^2 + (2\zeta\beta)^2]^{\frac{1}{2}}} \quad [3-47]$$

Here damping ratio, $\zeta = \frac{c}{2(m+A)\omega_0}$ and frequency ratio, β is the ratio between load frequency and natural frequency. x_{maks} is the maximum displacement and x_{static} is the static displacement due to load amplitude.

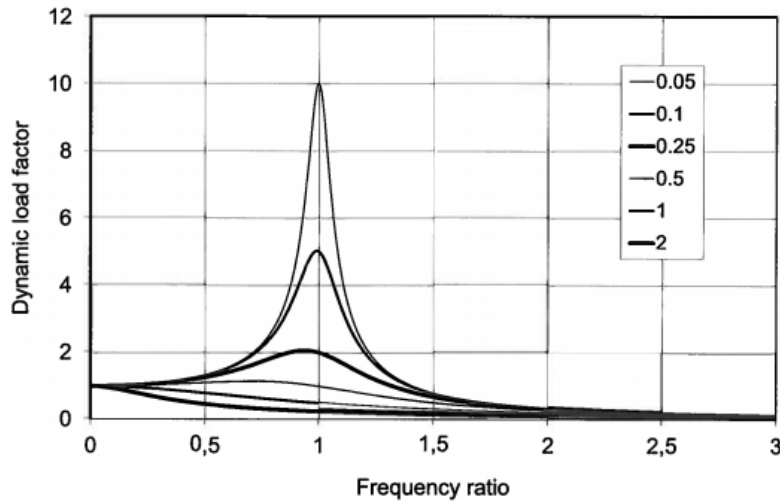


Figure 3-3 Dynamic load factor as function of the frequency ratio for given values of damping ratio (Larsen C. M., 2012)

Figure 3-3 illustrates the Dynamic load factor as function of the frequency ratio for given values of damping ratio and Figure 3-4 illustrates the corresponding diagram for phase angle. It is worth noting that phase angle lies between 0 to 180 degree, i.e. the response of the system is always after the external load in time.

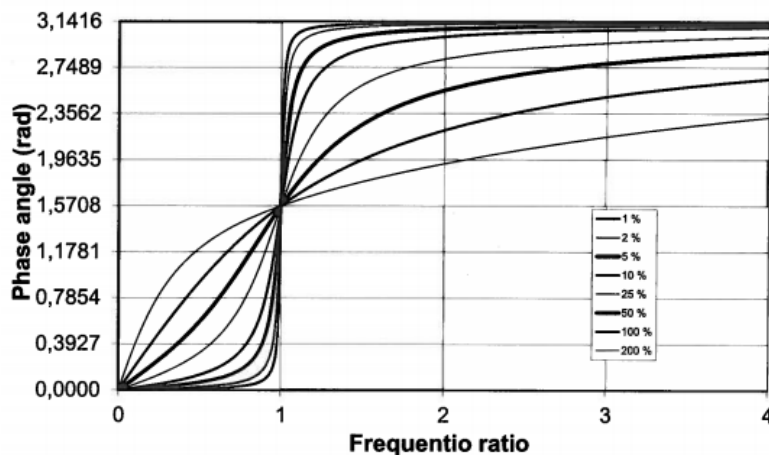


Figure 3-4 Phase angle between load and response as function of the frequency ratio for given values of damping ratio (Larsen C. M., 2012)

From Figure 3-3 we see that the maximum response for lightly damped system will increased dramatically when the load frequency approaches the natural frequency for, $\beta \rightarrow 1$. For $\beta > 1$ when $\omega > \omega_0$, the response will decrease with increasing β and for $\beta > 1.41$ dynamic response is less than static response.

Near the resonance where the load frequency is close or equal to natural frequency response is very high and there is a large variation due to change of damping. So, damping controls the response near resonance and damping is very important for low frequency motion because that is at resonance region. Because of this even though the magnitude of the low frequency force is lower than the wave frequency force, the response is higher.

The main sources of damping for LF motion are (Larsen K. , 2014):

- a) Viscous loads on floater's hull (skin friction and flow separation)
- b) Wave drift damping due to wave drift force change with floater velocity. When both waves and current exists the floater will experience additional damping, known as wave drift damping.
- c) Drag force on mooring line and riser
- d) Damping due to wind as wind force changes with floater velocity
- e) Damping from propeller and thrusters: Damping is tuned if automatic thruster assist is used

The linear damping coefficient C_l for mooring system is estimated based on measured or simulated time series of the horizontal turret force, F and the LF top end motion, x . The turret force can be assumed as:

$$F = m\ddot{x} + c\dot{x} + k_1x + k_2x^2 \quad [3-48]$$

where F is the total force, x , \dot{x} and \ddot{x} are LF surge position, velocity and acceleration. k_1 and k_2 are linear and quadratic stiffness respectively.

From the simulated or measured horizontal turret force and LF motion m , c , k_1 and k_2 can be calculated by minimizing the expected square error between the turret force and the model in equation [3-48]. The damping coefficient can be written as:

$$c = \frac{E(F \cdot \dot{x}) - k_1E(x \cdot \dot{x}) - k_2E(x^2 \cdot \dot{x})}{E(\dot{x}^2)} = \frac{E(F \cdot \dot{x})}{E(\dot{x}^2)} \text{ if } T \rightarrow \infty \quad [3-49]$$

where $E(\cdot)$ is the expected value operator. Total derivation of the above equation can be found in section 3.1.2 (Larsen & Ormberg, 1998)

3.4 Stiffness

The mooring lines have an effective stiffness composed of an elastic and geometrical stiffness as given in chapter 8 (Faltinsen, 1990). The elastic stiffness arises from the elastic properties of the cables and the geometric stiffness arises due to the change in mooring line geometry. The effective stiffness is found by the following equation.

$$\frac{1}{k_{effective}} = \frac{1}{k_{elastic}} + \frac{1}{k_{geometric}} \quad [3-50]$$

From the above equation we can understand that when $k_{geometric} \rightarrow \infty$ the total stiffness is governed by elastic stiffness (Figure 3-5) meaning that the line is totally stretched out and the stiffness is only provided by the material properties and when $k_{elastic} \rightarrow \infty$ the total stiffness is governed by geometrical stiffness (Figure 3-6) and comes from line characteristics.

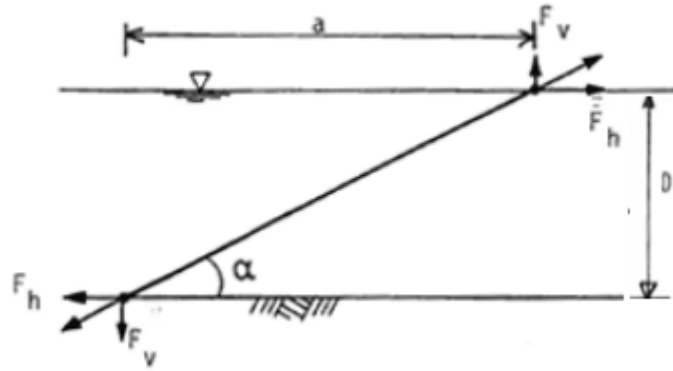


Figure 3-5 Elastic stiffness of mooring line (Larsen K. , 2014)

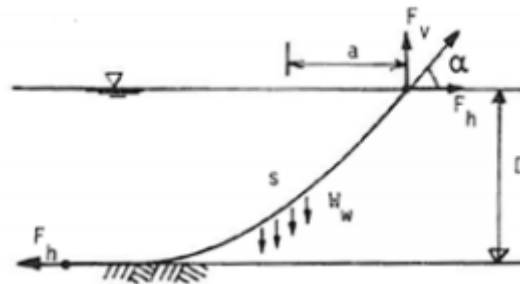


Figure 3-6 Geometrical stiffness of mooring line (Larsen K. , 2014)

The equilibrium of the line for elastic and geometrical stiffness is achieved by equation respectively (Larsen K. , 2014).

$$F_h \cdot D = F_v \cdot a ; \text{ for elastic stiffness} \quad [3-51]$$

$$F_h \cdot D = W_w \cdot a ; \text{ for geometric stiffness} \quad [3-52]$$

Here,

F_h – Horizontal force

F_v – Vertical force

W_w – Weight of mooring line

D – Vertical distance from fairlead to anchor

a – Horizontal distance from fairlead to anchor for elastic stiffness

a – Horizontal distance from fairlead to COG of line for geometric stiffness

For catenary chain and wire rope geometrical stiffness is more important and for polyester ropes elastic stiffness is dominating. For geometric stiffness the horizontal stiffness from one mooring line is determined by the line characteristics. A relation between the horizontal tension at the top end, T_x and the offset of the floating structure, X_l can be established both for inelastic and elastic line (Figure 3-7) using the catenary equation. The mooring lines are assumed to be without bending stiffness and when only gravity force is acting a freely

hanging homogeneous cable will assume the shape of catenary. The equations for calculating relation between T_x and X_l are taken from lecture notes (Larsen K. , 2014).

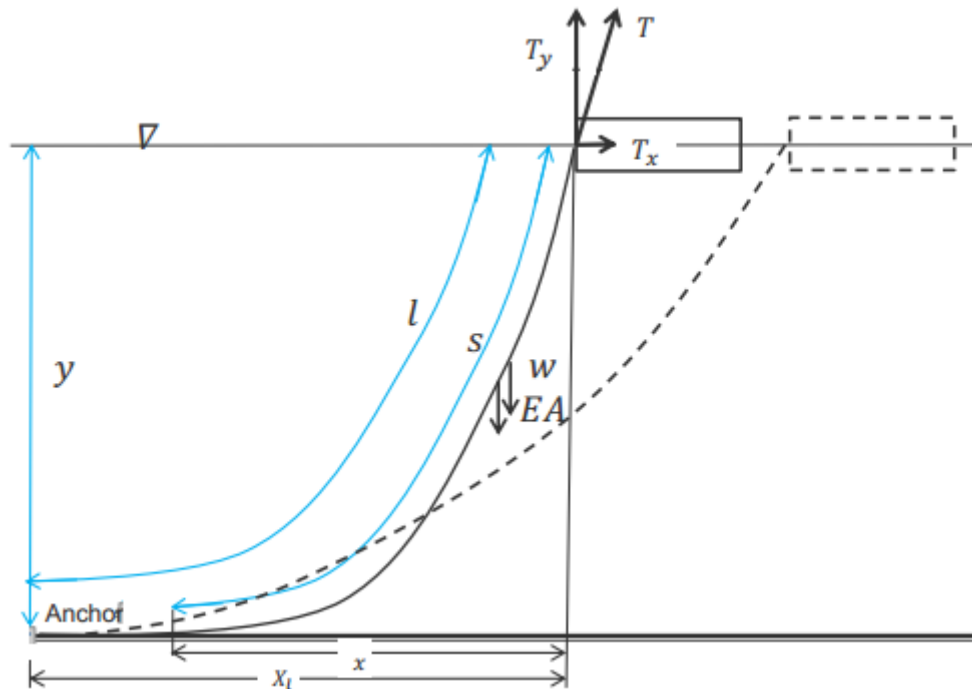


Figure 3-7 Horizontal stiffness from one mooring line (Larsen K. , 2014)

In the above figure following values are known and other values are calculated using the equations given below.

- Axial stiffness, EA
- Line weight, w
- Water depth, y
- Line length, l

For an inelastic line ($\frac{T}{EA} \ll 1$) the relation between T_x and X_l can be found by the following equation.

$$X_l = l + \frac{T_x}{w} \cdot \cosh^{-1} \left(1 + \frac{w \cdot y}{T_x} \right) - \sqrt{y \cdot \left(y + \frac{2T_x}{w} \right)} \quad [3-53]$$

For elastic line total tension is calculated from horizontal and vertical tension and the relation between tension and offset is found by equation [3-57].

$$T_x = EA \left[\sqrt{\left(\frac{T}{EA} + 1 \right)^2 - \frac{2wy}{EA}} - 1 \right] \quad [3-54]$$

$$T_y = w \cdot s \quad [3-55]$$

$$T = \sqrt{T_x^2 + T_y^2} \quad [3-56]$$

$$x = \frac{T_x}{w} \cdot \sinh^{-1} \left(\frac{T_y}{T_x} \right) + \frac{T_x \cdot T_y}{w \cdot EA} \quad [3-57]$$

3.5 Environmental loads to vessel motion

Contribution of the environmental loads to the vessel motion is given in Table 3-1 which shows that contribution of wind in the wave frequency range is ignored it is due to the fact that wind energy in this range is small compared to the 1st order wave energy. Current has only mean load as it is not considered as dynamic.

Table 3-1 Contribution of environmental loads to vessel motion

Vessel motion	Env. loads	Mean freq. load	Low freq. load (T = 70-200s)	Wave freq. load (T = 5-35s)
Horizontal, X	Waves	√ (mean wave drift)	√ (dynamic wave drift)	√ (1 st order wave)
	Wind	√ (Mean wind speed)	√ (Wind gust)	X
	Current	√	X	X
Vertical, Z	Waves	X	X	√

3.6 Design procedure – flow chart

Design procedure for mooring system follows several steps. Typically one can use the flow chart illustrated in Figure 3-8.

This iteration procedure has been followed in this thesis to get the intact mooring system which satisfies the ultimate limit state (ULS) condition meaning the required safety factor as mentioned in section 4.2 is achieved.

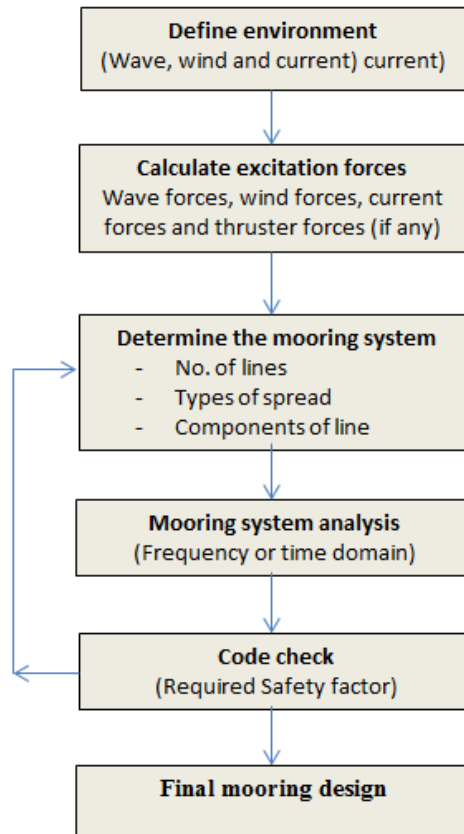


Figure 3-8 Iteration process for mooring system analysis

4 Rules and Regulation for Mooring

4.1 Design limit states

The mooring system shall be analyzed according to design criteria formulated in terms of three limit state equations (DNV, 2013):

- a) An ultimate limit state (ULS) to ensure that the individual mooring lines have adequate strength to withstand the load effects imposed by extreme environmental actions. We use worst sea state along the 100 year contour line ($q=0.01$) and the combine with 100 year wind and 10 year current. Also need to assess the weather directions especially for ships or FPSO.
- b) An accidental limit state (ALS) to ensure that the mooring system has adequate capacity to withstand the failure of one mooring line, failure of one thruster or one failure in the thruster's control or power systems for unknown reasons in extreme weather conditions (100 year returned period). A single failure in the control or power systems may cause that several thrusters are not working.
- c) A fatigue limit state (FLS) to ensure that the individual mooring lines have adequate capacity to withstand cyclic loading taking all possible sea states into account.

4.2 Required safety factors for ULS and ALS

Failure is most likely to occur if the load is unusually high and the strength is unusually low. In order to satisfy ULS and ALS condition all mooring lines need to satisfy the following equation (Larsen K. , 2014).

$$R_C \geq T_C \cdot sf \quad [4-1]$$

Here,

R_C – Characteristic strength which is the minimum breaking strength of the mooring line

T_C – Characteristic tension which is the most probable largest in the worst 100 year sea state (Figure 4-1)

sf – Safety Factor (Table 4-1 and Table 4-2)

In MIMOSA the safety factor is found by using equation [4-2]. They are calculated for all segments and the lowest value is selected for the whole line.

$$\text{Safety factor} = \frac{\text{Mooring line segment's breaking load}}{\text{Maximum tension occurring for that segment}} \quad [4-2]$$

Safety factors for station keeping system for floating offshore structures and mobile drilling units varies according to region.

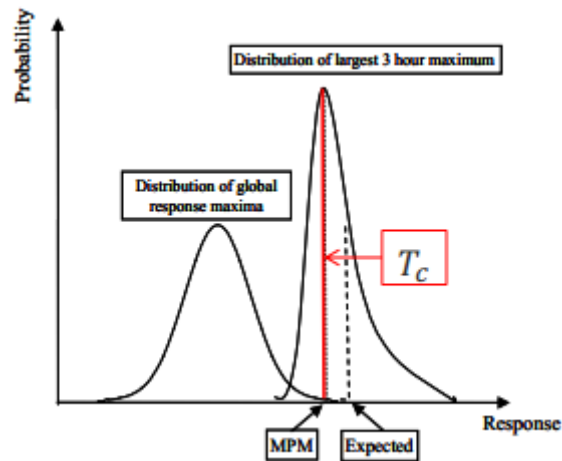


Figure 4-1 Characteristic Tension from probability distribution of tension

In Table 4-1 and Table 4-2 required safety factors are given for Permanent oil storage or production units and mobile drilling units respectively.

Table 4-1 Safety factors for permanent oil storage or production units (Larsen K. , 2014)

Weather condition	Intact (ULS)	One line failure (ALS1)	Two line failure (ALS2)
100 year returned period	Norway: 2.2	Norway: 1.5 International: 1.25	N/A
10 year returned period	N/A	N/A	Norway: 1.5 International: N/A

Table 4-2 Safety factors for mobile drilling units (Larsen K. , 2014)

Weather condition	Intact (ULS)	One line failure (ALS1)
100 year returned period	Norway: 1.9	Norway: 1.3
5-10 year returned period	International: 1.67	International: 1.25

4.3 FLS acceptance criteria for the Norwegian Continental Shelf (NCS)

Fatigue analysis is required for floating production facilities e.g. FPSO and flotels. It has been done for many years. In order to do the fatigue calculation one needs to follow the international standards and regulation requires that calculation should be based on (ISO 19901-7, 2013) chapter 9. According to section 8.1.2.5 of (ISO 19901-7, 2013), fatigue analysis is not required for MODUs.

DNV also have acceptance criteria for fatigue calculation. According to (DNV, 2013) the fatigue limit state is intended to ensure that each type of component in an individual mooring line has a suitable resistance to fatigue failure. The design equation for FLS is:

$$1 - d_c \cdot \gamma_F \geq 0 \quad [4-3]$$

Here,

d_c = the characteristic fatigue damage accumulated as a result of cyclic loading during the design life time. The combined spectrum approach or the dual narrow band shall be applied as the cycle counting algorithms (section 5.1.2).

γ_F = the single safety factor for the fatigue limit state.

$$\gamma_F = 5 ; \text{ when } d_F \leq 0.8 \quad [4-4]$$

$$\gamma_F = 5 + 3 \cdot \left(\frac{d_F - 0.8}{0.2} \right); \text{ when } d_F > 0.8 \quad [4-5]$$

Where d_F is the adjacent fatigue damage ratio, which is the ratio between the characteristic fatigue damage d_c in two adjacent lines taken as the lesser damage divided by the greater damage.

5 Fatigue Assessments

There are several methods for calculating fatigue damage in mooring line. These methods are well described in section 9.3.2 and 9.3.3 (ISO 19901-7, 2013) and chapter 6 (DNV, 2013). The content in this chapter are mostly taken from DNV-OS-E301 (DNV, 2013).

The characteristic fatigue damage (d_c), accumulated in a mooring line component as a result of cyclic loading, is summed up from the fatigue damage arising in a set of environmental states in a long term analysis that the mooring system is subjected to:

$$d_c = \sum_{i=1}^{i=n} d_i \tag{5-1}$$

Where d_i is the fatigue damage to the component arising in state i (total sea states discretize into $i=1, \dots, n$ states)

In a stress history of several stress ranges $S_{r,i}$, each with a number of cycles n_i , the damage sum follows from the following equation according to Miner-Palmgren rule,

$$D = \sum_i \frac{n_i}{N_i} \tag{5-2}$$

Here N_i is the total number of cycles required to failure from S-N curve for specific stress range. The summation procedure is illustrated in Figure 5-1.

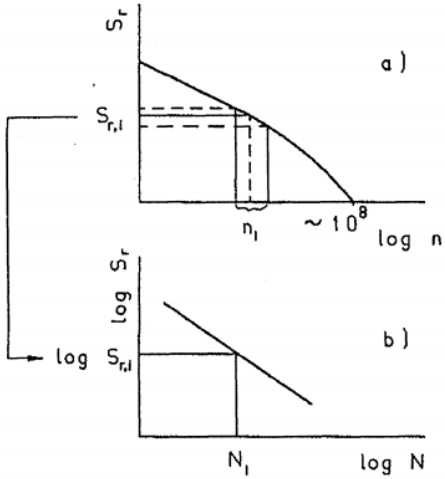


Figure 5-1 The Miner summation procedure; (a) stress range (b) S-N curve (Berge, 2006)

When the effects of mean tension are neglected, the fatigue damage accumulated in a individual state may be computed as:

$$d_i = n_i \int_0^{\infty} \frac{f_{Si}(s)}{n_c(s)} ds \quad [5-3]$$

Where n_i is the number of stress cycles encountered in state i , $f_{Si}(s)$ is the probability density of the nominal magnitudes (peak-to-trough) of stress cycles applied to the component in state i , and $n_c(s)$ is the number of stress cycles of magnitudes that would lead to failure of the component.

The nominal magnitudes of the corresponding tension cycles by the nominal cross-sectional area of the component; i.e. $\frac{2\pi d^2}{4}$ for chain, and $\frac{\pi d^2}{4}$ for steel wire rope, where d is the component diameter.

The number of stress cycles in each state is usually determined as:

$$n_i = v_i \cdot P_i \cdot T_D \quad [5-4]$$

Where, v_i = the mean-up-crossing rate (in hertz) of the stress process,

P_i = the probability of occurrence of state i , and

T_D = the design lifetime of the mooring line component in seconds.

For the component capacity against tension fatigue S-N curves are used. The parameters a_D and m of the S-N curves and the S-N curves are given in Table 5-1 and Figure 5-2 respectively.

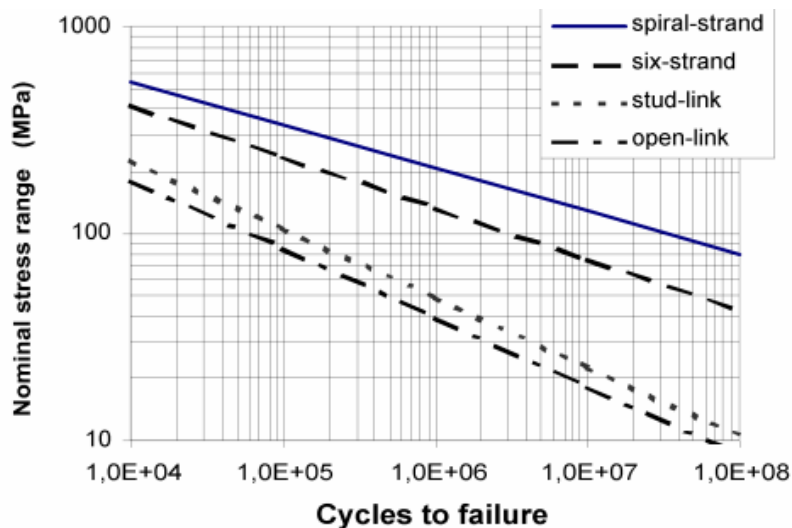


Figure 5-2 Design S-N curves for Mooring lines (DNV, 2013)

Table 5-1 S-N fatigue curve parameters (DNV, 2013)

	a_D	m
Stud chain	$1.2 \cdot 10^{11}$	3.0
Studless chain (open link)	$6.0 \cdot 10^{10}$	3.0
Stranded rope	$3.4 \cdot 10^{14}$	4.0
Spiral rope	$1.7 \cdot 10^{17}$	4.8

5.1 Frequency response method

5.1.1 Simple summation approach (SS)

If the low-frequency content of the stress process is negligible, then a narrow-banded assumption may be applied and fatigue damage is calculated by the following equation.

$$d_{NBi} = \frac{v_{0i}T_i}{a_D} (2\sqrt{2}\sigma_{Si})^m \Gamma\left(\frac{m}{2} + 1\right) \quad [5-5]$$

Where σ_{Si} is the standard deviation of the stress process, the duration of the environmental state, $T_i = P_i \cdot T_D$.

Using the above equation LF and WF fatigue damage are calculated independently and sum of them is the total damage. If both wave frequency and low frequency components are significant the following alternatives are recommended to use.

5.1.2 Combined spectrum approach (CS)

The combined spectrum approach may be used in computing the characteristic damage which is relatively simple and conservative. The fatigue damage for one sea states is obtained by the following equation.

$$d_{Csi} = \frac{v_{yi}T_i}{a_D} (2\sqrt{2}\sigma_{Yi})^m \Gamma\left(\frac{m}{2} + 1\right) \quad [5-6]$$

Here, σ_{Yi} includes both WF and LF components and is computed using $\sigma_{Yi} = \sqrt{\sigma_{Li}^2 + \sigma_{Wi}^2}$.

The mean-up-crossing rate v_{yi} in hertz is computed from the moments of the combined spectrum:

$$v_{yi} = \sqrt{\lambda_{Li}v_{Li}^2 + \lambda_{Wi}v_{Wi}^2} \quad [5-7]$$

λ_L and λ_W are defined by,

$$\lambda_L = \frac{\sigma_L^2}{\sigma_L^2 + \sigma_W^2}; \lambda_W = \frac{\sigma_W^2}{\sigma_L^2 + \sigma_W^2}, \quad [5-8]$$

5.1.3 Dual narrow band approach (DNB)

The dual narrow-banded approach takes the result of the combined spectrum approach and multiplies it by a correction factor ρ , based on the two frequency bands that are present in the tension process.

$$d_{DNBi} = \rho_i \cdot d_{CSI} \quad [5-9]$$

The correction factor can be found by,

$$\rho = \frac{v_P}{v_y} \left[(\lambda_L)^{\frac{m}{2}+2} \left(1 - \sqrt{\frac{\lambda_W}{\lambda_L}} \right) + \sqrt{\pi \lambda_L \lambda_W} \cdot \frac{m \Gamma\left(\frac{1+m}{2}\right)}{\Gamma\left(\frac{2+m}{2}\right)} \right] + \frac{v_W}{v_y} \cdot (\lambda_W)^{\frac{m}{2}} \quad [5-10]$$

And the mean-up-crossing rate is given by,

$$v_P = \sqrt{\lambda_L^2 v_L^2 + \lambda_L \lambda_W v_W^2 \delta_W^2} \quad [5-11]$$

Here δ_W is the bandwidth parameter for the wave frequency part of the stress process. According to (DNV, 2013) it is set as 0.1.

5.2 Time domain analysis

5.2.1 Weibull approach

Weibull approach is derived from closed form fatigue life equations. A detail discussion on this approach is given in (Almar-Næss, 1985). It is assumed that a structural detail is subjected to n_0 stress cycle in total and these stress cycles are randomly distributed with a probability distribution function. For offshore structures the probability density function of stress range may be represented by a two parameter Weibull-distribution. Using these assumptions the following equation can be derived to calculate fatigue damage.

$$D = \frac{n_0}{a_D} \cdot (q)^m \cdot \Gamma\left(\frac{m}{h} + 1\right) \quad [5-12]$$

where h and q are Weibull parameters.

The shape of the long term distribution of stress ranges may vary due to different values of h parameter as shown in the following figure.

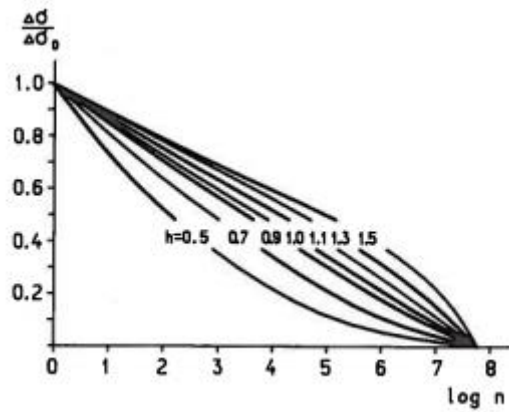


Figure 5-3 Long term distribution of stress range (Almar-Næss, 1985)

It is convenient to eliminate the Weibull parameter q by introducing the maximum stress range $\Delta\sigma_0$ during n_0 number of cycles and we get the following equation for calculating fatigue damage.

$$D = \frac{n_0}{a_D} \cdot \frac{\Delta\sigma_0^m}{(\ln n_0)^{\frac{m}{h}}} \cdot \Gamma\left(\frac{m}{h} + 1\right) \quad [5-13]$$

This expression implies:

- a. The Miner-Palmgren rule
- b. An S-N curve with no cut-off level
- c. The two parameter Weibull distribution for the probability density function of stress ranges
- d. $\Delta\sigma_0$ is the maximum stress range for a total of n_0 cycles.
- e. h is the Weibull parameter describing the shape of the long term stress range distribution.

5.2.2 Rain-flow counting approach (RFC)

In this approach rain-flow counting method is used to estimate the number of tension cycles and the expected value of the tension ranges from a time history of tension. The tension time history may be determined directly by a time domain mooring analysis or it may be generated from the combined low and wave frequency tension spectrum.

The counting procedure is designed to count reversals in accordance with the material's stress-strain response and each time the hysteresis loop is closed, a cycle count is made. Small cycles within the large cycles are also counted thus reflecting the way in which the material is responding. The principle may be illustrated in Figure 5-4.

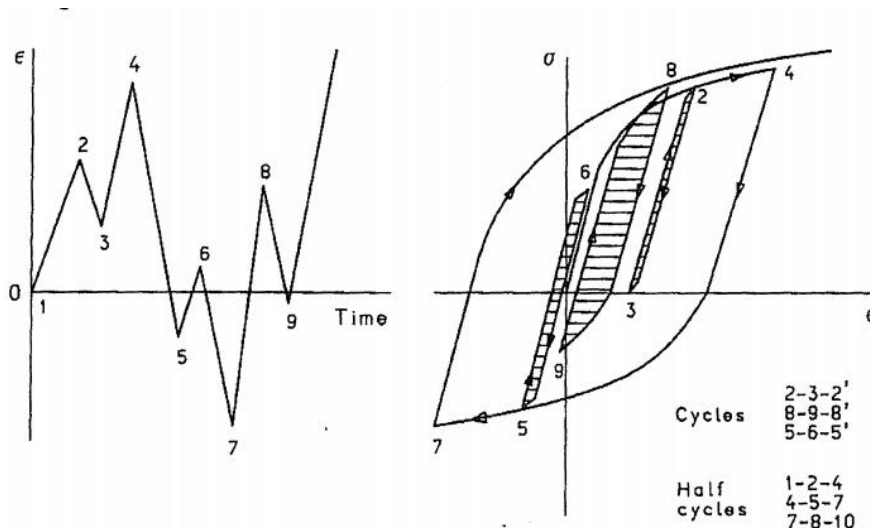


Figure 5-4 Rain-flow cycle counting procedure (Berge, 2006)

After performing rain-flow counting the total damage can be calculated using Miner-Palmgren rule (equation [5-2]).

There is fairly general consensus that the rain-flow counting technique provides the most accurate estimate for fatigue damage if rigorously performed with sufficient number of time simulations representative of the wave scatter diagram. But it is relatively time-consuming analysis.

5.3 Fatigue analysis procedure

The recommended practice 2SK by (API, 2005) describes a fatigue analysis procedure for mooring line in section 6.4. The procedure will be briefly presented in this chapter. The fatigue analysis is calculated by the following steps.

- i. The long term environmental conditions can be represented by a number of discrete design conditions. Each condition consists of a reference direction and a reference sea state which is characterized by:
 - a. A significant wave height and peak period
 - b. Current velocity
 - c. Wind velocity

The probability of occurrence of these conditions must be specified and 8 to 10 reference direction is needed for the directional distribution of a long term environment. Total number of reference sea states should be in the range of 10 to 50 as the damage prediction is sensitive to the number of sea states.

- ii. Each condition can be analyzed analogously to the procedure used for ULS condition in section 5 (API, 2005). The wave frequency tension can be computed about the position of the mooring system under mean loading only. The method given in the guidance note in section 6.3.3 (DNV, 2013) can be used which consists of the following steps.
 - a) Determine all loads and motions (low and wave frequency).

- b) Compute mooring system responses under mean loading using quasi-static analysis and then impose wave frequency motions and calculate σ_{WF} from dynamic analysis.
- c) Add σ_{LF} to the mean position and calculate the corresponding tension and σ_{LF} is the calculated tension minus the tension in mean position.
- iii. Determine the T-N curve applicable to the mooring line
- iv. Compute the annual damage from one environmental condition due to both low frequency and wave frequency tension using one of the following methods.
 - a) Simple summation (SS)
 - b) Combined spectrum (CS)
 - c) Dual narrow-band (DNB)
 - d) Rain flow counting (RFC)
- v. Repeat step (iv) for all environmental conditions and calculated the corresponding fatigue damage.
- vi. Calculate the annual fatigue damage D and fatigue life L for all mooring lines.

5.4 Parameters for comparison of fatigue damage

In order to compare difference between two analysis methods 1st we need to find out which parameter is important for checking. Using the equation [5-6] we can calculate the fatigue damage for two different conditions as given below.

$$d_{CS1} = \frac{v_{y1}T_1}{a_D} (2\sqrt{2}\sigma_{Y1})^m \Gamma\left(\frac{m}{2} + 1\right) \quad [5-14]$$

$$d_{CS2} = \frac{v_{y2}T_2}{a_D} (2\sqrt{2}\sigma_{Y2})^m \Gamma\left(\frac{m}{2} + 1\right) \quad [5-15]$$

The ratio of damage between these two conditions can be found by:

$$\frac{d_{CS1}}{d_{CS2}} = \frac{\frac{v_{y1}T_1}{a_D} (2\sqrt{2}\sigma_{Y1})^m \Gamma\left(\frac{m}{2} + 1\right)}{\frac{v_{y2}T_2}{a_D} (2\sqrt{2}\sigma_{Y2})^m \Gamma\left(\frac{m}{2} + 1\right)} \quad [5-16]$$

If both of them use the same S-N curve the value of a_D and m will be same and the ratio becomes:

$$\frac{d_{CS1}}{d_{CS2}} = \frac{v_{y1}T_1(\sigma_{Y1})^m}{v_{y2}T_2(\sigma_{Y2})^m} \quad [5-17]$$

The standard deviation of the stress process and the mean-up-crossing rate of a sea state can be found using standard deviation of the tension process (σ_{Ti}) and the mean-up-crossing period (t_{zi}):

$$\sigma_{Yi} = \frac{\sigma_{Ti}}{A} \text{ and } v_{yi} = \frac{1}{t_{zi}} \quad [5-18]$$

Using the above equation we can write:

$$\frac{d_{CS1}}{d_{CS2}} = \frac{\frac{1}{t_{z1}} T_1 \left(\frac{\sigma_{T1}}{A}\right)^m}{\frac{1}{t_{z2}} T_2 \left(\frac{\sigma_{T2}}{A}\right)^m} \quad [5-19]$$

If the damage is calculated for same line and same duration of sea state A and T will be also the same and m value is same for same S-N curve. So, we can write:

$$\frac{d_{CS1}}{d_{CS2}} = \frac{t_{z2}}{t_{z1}} \cdot \left(\frac{\sigma_{T1}}{\sigma_{T2}}\right)^m \quad [5-20]$$

From the above equation it is evident that standard deviation of the tension process (σ_T) and the mean-up-crossing period (t_z) are the parameters that will be responsible for the differences in results. But the ratio of σ_T is more important as it is raised to the power of m and the fatigue damage ratio will also vary significantly if the difference between two standard deviation σ_T is high.

6 Model Description

6.1 Vessel description

6.1.1 Main particulars and layout

For the case study Åsgard A FPSO is selected which is shown in Figure 6-1. The FPSO was delivered by Aker Solutions as a complete engineering, procurement and construction (EPC) contract and is based on the Tentech 900 design by Aker Solutions for the Åsgard field. The Åsgard field lies on the Halten Bank in the Norwegian Sea, at a water depth of 320m and about 200 kilometers off mid-Norway. The Åsgard A FPSO measures 278m in length and has a displacement of 184 300t.



Figure 6-1 Åsgard A FPSO

Main particulars of the vessel are given in the following table.

Table 6-1 Main particulars of Åsgard A FPSO

Vessel Name	Åsgard A FPSO
Length over all	276.4 m
Length between perpendicular	258 m
Breadth moulded	45.4 m
Depth	26.6 m
Mean draught	16.5 m
Displacement	173.5 ton
Turret position from CG to forward Turret (original)	36.6 m
Turret position (modified for thesis)	100 m

6.1.2 Hydrodynamic properties

Vessel file is directly taken as a SIMA input file from the output file of WADAM. It contains all the data related to current force coefficient, wave drift force coefficient, wind forces coefficient and RAO's. But as it is a output file from software it is better to check it before using it and also the definition for directions of wind, wave and current needs to be checked. All the forces and RAO's are plotted and they are given in APPENDIX D. From the plots following characteristics are found.

Current force coefficient: Current force coefficients are based on equation [3-43]. Some of the important characteristics of this coefficient for the chosen vessel is given below.

- Values are highest when current directions are 0 or 180 degree and they are symmetric around the bow.
- For surge motion they are highest when coming from transverse direction meaning 90 and 270 degree (Figure 6-2).
- For yaw the values are zero for 0, 90, 180 and 270 degree as the arm for moment is zero.

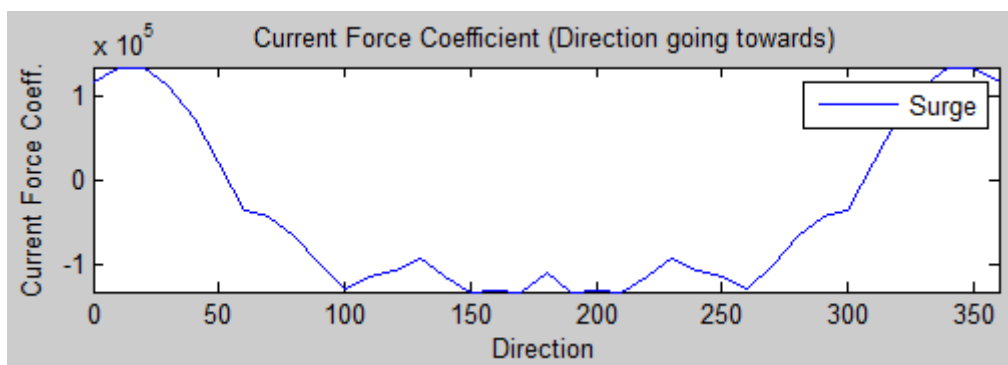


Figure 6-2 Current force coefficient (Direction - going towards)

Wind force coefficient: Wind force coefficient are based on equation [3-39] and as there is not that much variation in the superstructure it has same characteristic of the current force coefficient just the direction is opposite (Figure 6-3).

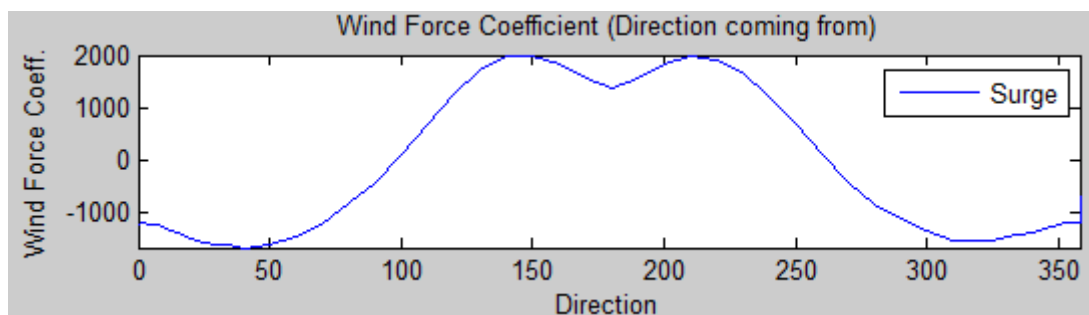


Figure 6-3 Wind force coefficient (Direction - coming from)

Properties of RAO's: Following properties are evident for the RAOs at center of gravity (COG) of FPSO.

- Near resonance (period 10.5s and frequency 0.598 rad/s) heave response is highest and for long waves (very low frequency) it becomes 1 as shown in the middle curve of Figure 6-4.
- RAO for pitch for very low frequency is close to 1 meaning that for 0 degree wave heading and large period of waves, the ship will follow the waves (last curve of Figure 6-4).
- It was also found that heave and pitch is 90 degree out of phase.

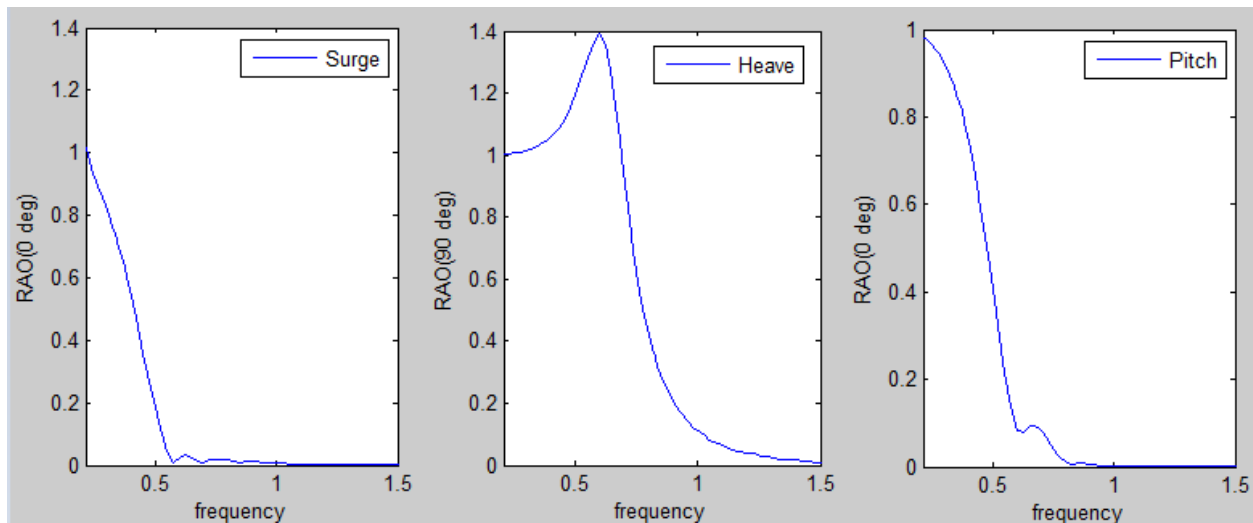


Figure 6-4 RAOs for surge, heave and pitch

Wave drift force coefficient: Water plane area controls the wave drift force as it controls the reflected waves. Three checks are done to verify whether the drift force coefficients are correct:

- 1st check: For very low frequency there should be no drift
- 2nd check: For high frequency (short waves) coefficient will have flat asymptotic values
- 3rd check: High motion creates more drift force and near heave frequency they have higher values.

Another characteristic is that sway drift force will be higher than the surge as the length of the vessel is higher than beam and sway drift acts in that direction.

6.2 Environmental loads

In this thesis the contour line concept is used, i.e. the 100-year design storm is taken as the most unfavorable sea state along the 100-year contour line. The duration of the sea state is taken to be 3-hours, and as an estimate of the 100-year response, the 90% fractile of the 3-hour extreme value distribution is recommended. If structure essentially behaves quasi statically the design wave concept can be adequate. All the values for environmental loads are taken from Heidrun metocean design basis (Statoil, 2004). The scatter diagram given in Table 6-2 is a modified scatter diagram of the original scatter diagram from (Statoil, 2004) to reduce the total number of sea states for long term analysis.

Table 6-2 Modified scatter diagram of sea states

Hs\Tp	3-5	5-7	7-9	9-11	11-13	13-15	15-17	17-19
0-2	2659	11124	13838	8642	3696	1286	401	119
2-4	113	3157	11558	13818	8384	3344	1029	271
4-6	0	42	977	3596	4129	2170	674	148
6-8	0	0	19	372	1163	1050	391	77
8-10	0	0	0	10	134	295	174	37
10-12	0	0	0	0	6	42	53	18
12-14	0	0	0	0	0	2	9	6
SUM	2772	14323	26392	26438	17512	8189	2731	676

The Directional probability is given in Table 6-3. An important assumption is that H_s and T_p values are same for all environmental direction.

Table 6-3 Direction probability of environmental loads (Statoil, 2004)

Direction	0	30	60	90	120	150	180	210	240	270	300	330
prob.	0.156	0.075	0.021	0.025	0.02	0.009	0.015	0.111	0.224	0.127	0.094	0.123

Wave loads for ULS: From figure below 100 year extreme value we choose for 1st checking mooring line integrity is 16 m H_s and 18.2s T_p and I have used the double peak spectrum. Then other seastate are checked along the 100 year contour line.

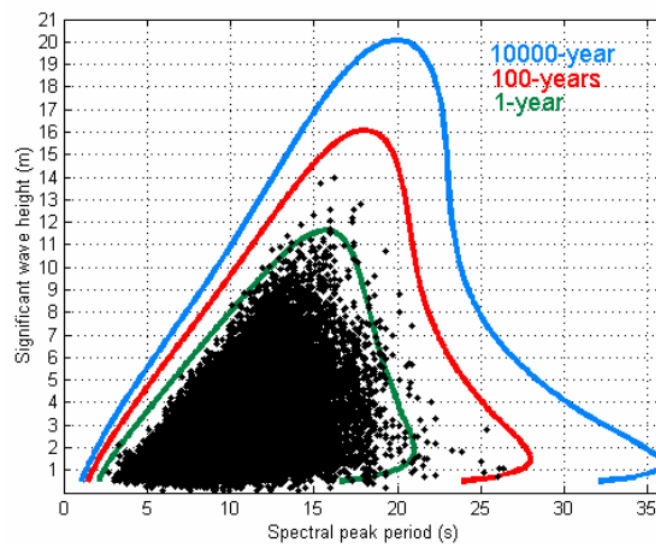


Figure 6-5 Heidrun 1, 10, 100 and 10000-year extreme contour lines in H_s – T_p plane (Statoil, 2004)

(Sea state duration: 3 hours)

Wind loads for ULS: Extreme wind speeds 36 (m/s) with 100 year return period for 1h averaging time intervals 10 m above SWL.

For long term simulation wind velocity for all sea states is used same as extreme wind speeds for ULS condition which is conservative. In reality it should vary with sea state condition (H_s).

Current loads for ULS: From table 4.1 of metocean data 10 year return period current speed is 0.94 m/s for surface current.

6.3 Mooring lines properties

The mooring file comprises of 12 mooring lines and all the lines have same characteristics. Pretension and diameter of the line is changed in order to get the final mooring system. Diameter and breaking strength of stud less chain R4 is taken from the technical brochure of Ramnas (Ramnäs, 2014) and for steel wire rope relevant values are taken from Heidrun design basis and scaled accordingly to get the required dimension of steel wire rope. To get the modulus of elasticity for studless chain R4, (E) equation [6-1] is used from (DNV, 2013).

$$E = (5.45 - 0.0025 \cdot D) \cdot 10^{10} \text{ N/m}^2 \quad [6-1]$$

For spiral ropes it is $1.13 \times 10^{10} \text{ N/m}^2$ corresponding to the nominal diameter of the wire rope.

Table 6-4 Properties of mooring lines

Segment	Diameter (m)	Segment Length (m)	Nb. of elements	Modulus of elasticity	Unit weight In water (N/m)	Drag coeff. in normal dir.	Breaking strength (kN)
1 Chain	0.137	930.0	30	5.105e+07	3.197	2.4	16992
2 Chain	0.142	285.0	30	5.095e+07	3.427	2.4	18033
3 Wire	0.147	300.0	20	1.130e+08	0.787	1.8	18000
4 Chain	0.147	52.0	10	5.085e+07	3.680	2.4	19089

*segment number starts from anchor.

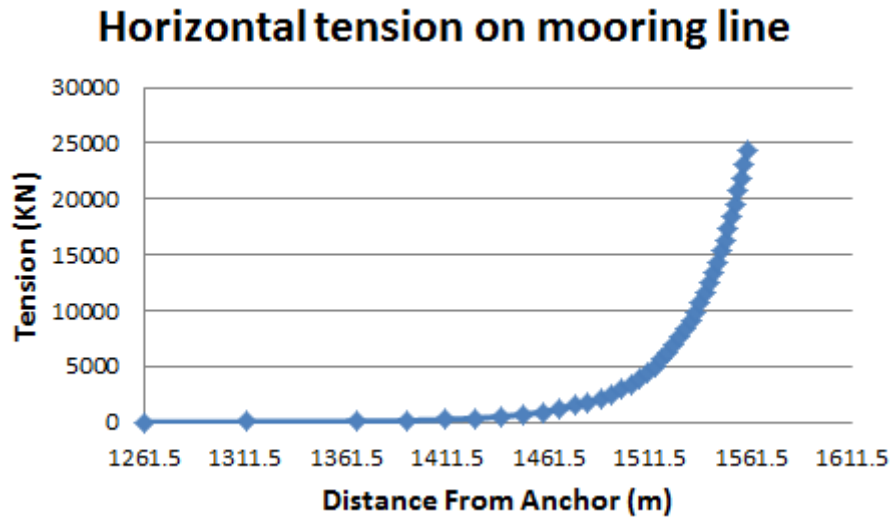


Figure 6-6 line characteristics curve indicating horizontal tension vs. distance to anchor

Line characteristic for all mooring line is shown in Figure 6-6 which is same for all lines as the lines are evenly spread.

6.4 MIMOSA Model

The vessel file in MIMOSA model is taken as output from SIMA model and the same mooring file is used as in the master project (Saidee, 2014). The mooring file is attached in APPENDIX C. Definition of directions associated with force coefficients and transfer functions in the MIMOSA file is shown in Figure 6-7. Directions of waves and wind are coming from while the direction of current is going towards.

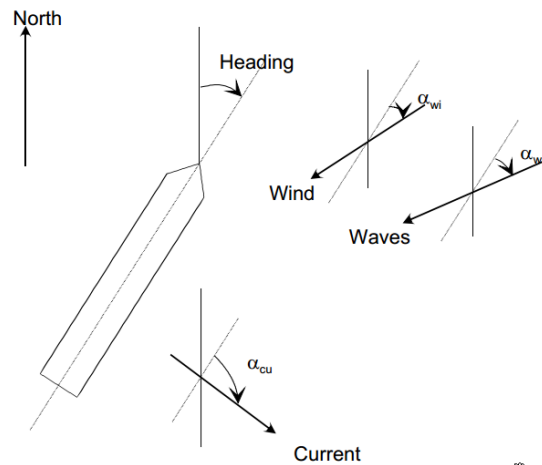


Figure 6-7 Definition of directions for force coefficients and RAOs in MIMOSA file

The old form of the long term simulation (LTS) input file is used to create the environmental file for all sea states. For each environmental condition the LTS input file contains a line with the following data given in Figure 6-8 Old form of LTS input of environmental file Figure 6-8.

T1 T2 T3 T4 T5 WINVEL WINDIR HS TP WAVDIR CURVEL CURDIR

T1, ... ,T5	Variables which can be used to identify the condition (number, time, date etc.)	R	
WINVEL	Wind speed (m/s)	R	
WINDIR	Wind propagation direction in global coordinate system (deg)	R	
HS	Significant wave height (m)	R	
TP	Peak period (s)	R	
WAVDIR	Wave propagation direction in global coordinate system,(deg)	R	
CURVEL	Current speed (m/s)	R	
CURDIR	Current propagation direction in global coordinate system (deg)	R	

Figure 6-8 Old form of LTS input of environmental file (MIMOSA, 2012)

The horizontal and vertical projections of the mooring lines are given in the figure which is plotted using MIMOSA software.

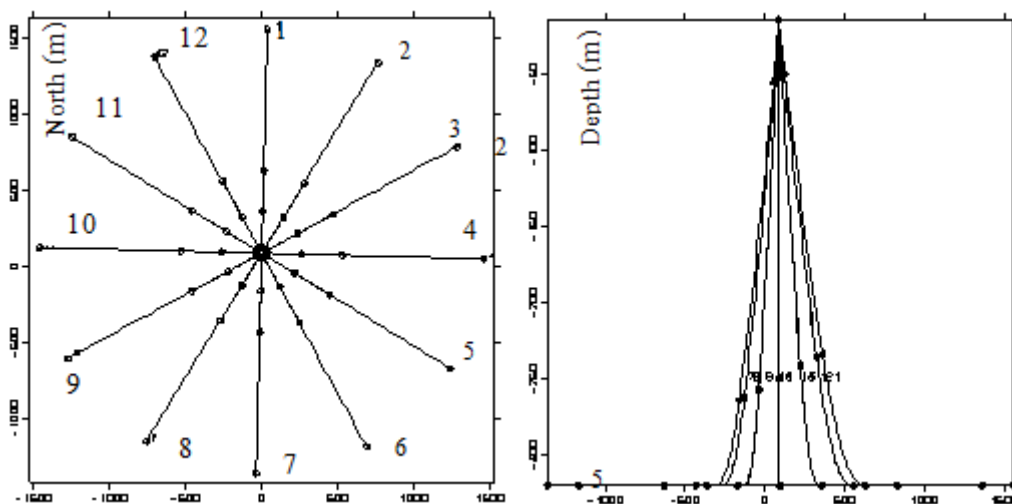


Figure 6-9 Horizontal (right) and vertical (left) projections of the mooring lines

The long term simulation was performed using macro file LONGTERM.MAC which is also given in APPENDIX C.

6.5 SIMA simulation model

At the beginning of thesis the intension was to use the same mooring file and vessel file from the master project (Saidee, 2014) and then use those files to create model in SIMA. But the

added mass in MIMOSA has no coupling terms on LF motion only in WF motion. Also first order motion transfer function is absent in the file as it is only for frequency domain analysis. Therefore, the vessel file for SIMA is used provided by Vegard Øgård Aksnes from MARINTEK instead of MIMOSA vessel file. But the mooring file from MIMOSA is used to create mooring system in SIMA and it worked perfectly well.

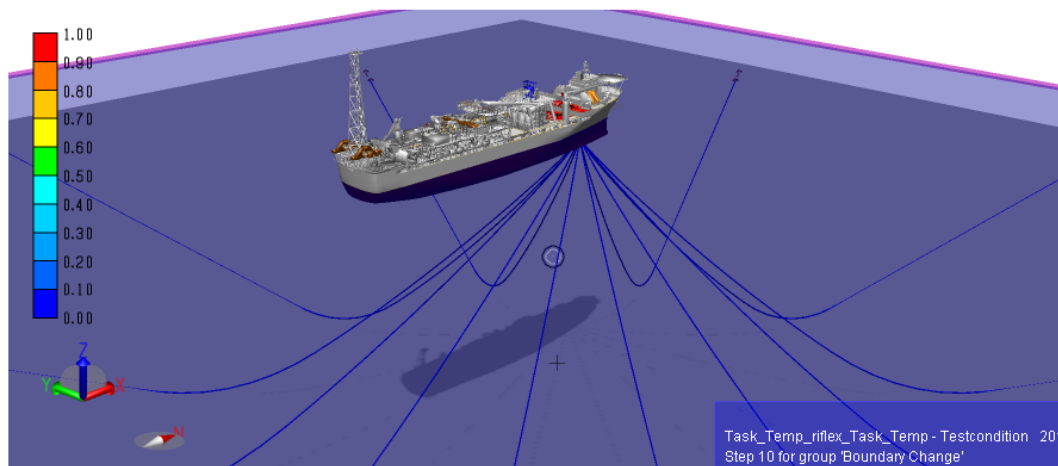


Figure 6-10 SIMA simulation model

Figure 6-10 illustrates the simulation model for fatigue analysis in time domain using rain flow counting method. SIMA is more user friendly program in terms of visualization and it is possible to check graphically if the model is correct.

In case of SIMA coupled time domain analysis is performed meaning that vessel and mooring is simulated simultaneously in a complete model of both the vessel (large body hydrodynamics) and the mooring system (finite element slender model). Both vessel motions and mooring line tensions are simulated simultaneously.

6.6 Model verification

In this thesis two different software packages are used. So, the simulation models in both software need to be equivalent and also the environmental loads should act on the system in similar manner. Before doing the comparison study we need to ensure that the differences only arises from the computational difference within the software, not due to the modeling errors. Static results are mainly used for verification process and it was carried out early in the modeling stage.

Figure 6-11 shows the restoring forces of mooring system due to change in offset distance for both the SIMA and MIMOSA model and they corresponds very well meaning both models are acting in a similar manner.

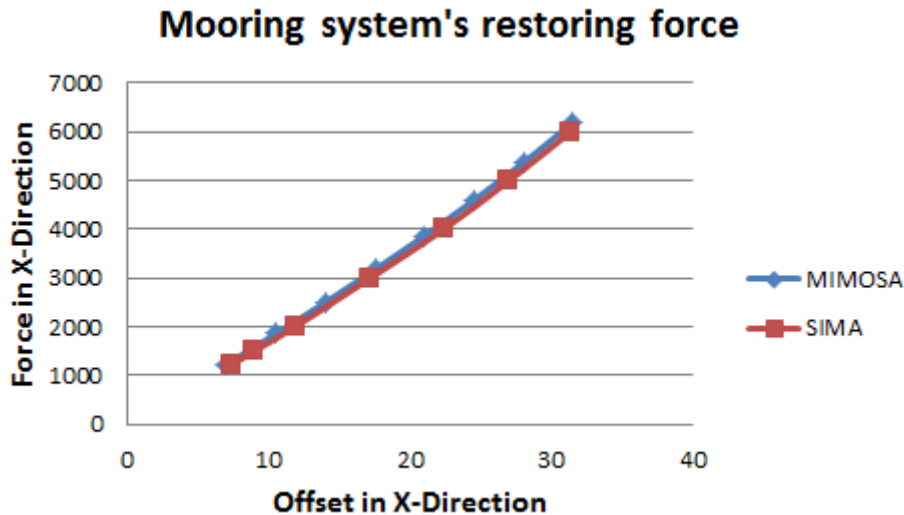


Figure 6-11 Comparison of restoring force in SIMA and MIMOSA model

Equilibrium position with respect to the vessel COG, calculated by the MIMOSA and SIMA for the same sea state ($H_s = 9\text{m}$ and $T_p = 14\text{s}$) is given in the following table and we can see that the deviation is not that significant. In case of surge offset the deviation is 4%.

Table 6-5 Equilibrium position of vessel from MIMOSA and SIMA

Software	Surge (m)	Sway (m)	Yaw (Degree)
MIMOSA	11.92	2.3	1.46
SIMA	12.4	1.89	1.12

It was also checked whether the environments loads applied in both the software are of the same magnitude or the deviation is in the allowable range. In Table 6-6 all the environmental loads that are applied in MIMOSA and SIMA for sea state ($H_s = 9\text{m}$ and $T_p = 14\text{s}$) and the deviation is calculated with respect to the MIMOSA results. One can see that there is only slight deviation between the applied loads in two models.

Table 6-6 Environmental loads in X-direction (surge) from MIMOSA and SIMA

Load types	MIMOSA	SIMA	Deviation (%)
Wind load (kN)	1497	1504	0.46
Wave load (kN)	521.5	529	1.43
Current load (kN)	100.9	100.3	-0.59
Total load (kN)	2119.6	2133	0.63

6.7 Important issues during modeling (errors and solutions)

In MIMOSA the modeling is comparatively easy than the SIMA. During the simulation stage in SIMA several errors were found. In this chapter two important errors will be discussed along with their solutions.

6.7.1 Error related to drag coefficient

Another important issue was that the mooring lines were experiencing load cycles of very high frequency as shown in figure below. Finally it was found that this occurred as there was no longitudinal drag coefficient, C_D given for the mooring lines. After inserting the value of longitudinal C_D for mooring line components according to table 1-1 of section 2.7.1 (DNV, 2013) this issue was solved.

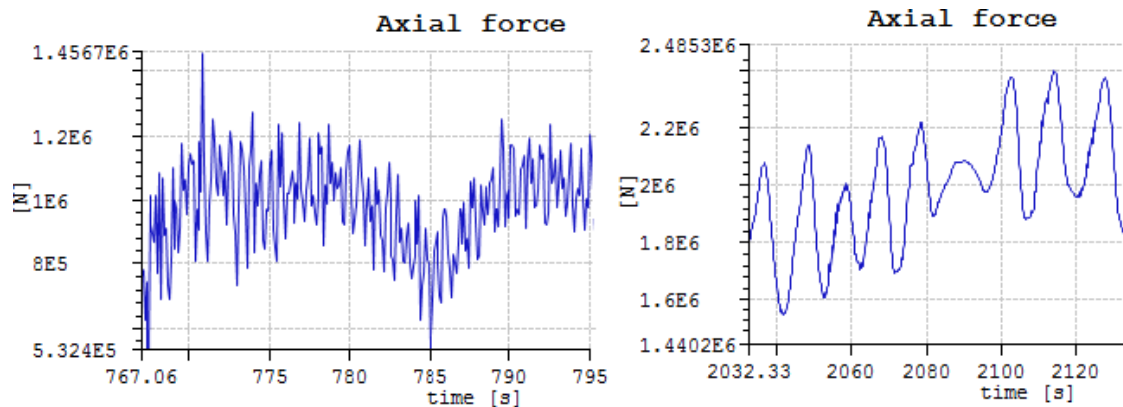


Figure 6-12 Time history of axial force of mooring line without (right) and with (left) longitudinal drag coefficient

6.7.2 Error related to modeling of leeward line of ship shaped units

One of the important issues during modeling of the mooring lines for ship shaped units e.g. FPSO is to model the leeward line. The reason is that when the line goes to slack the tension values can be zero meaning the line will have no stiffness as there is almost no pretension present. Numerical error in the time domain calculation may occur due to this.

For our case when doing the time domain simulation the using time step 0.1s the simulation used to fail for large sea states.

After discussing with Pål Levold from MARINTEK we have found that RIFLEX diverges because of compression in the leeward lines. In the screenshot given in Figure 6-13 we can see compression pulsations (red regions) in one mooring line just before the simulation fails.

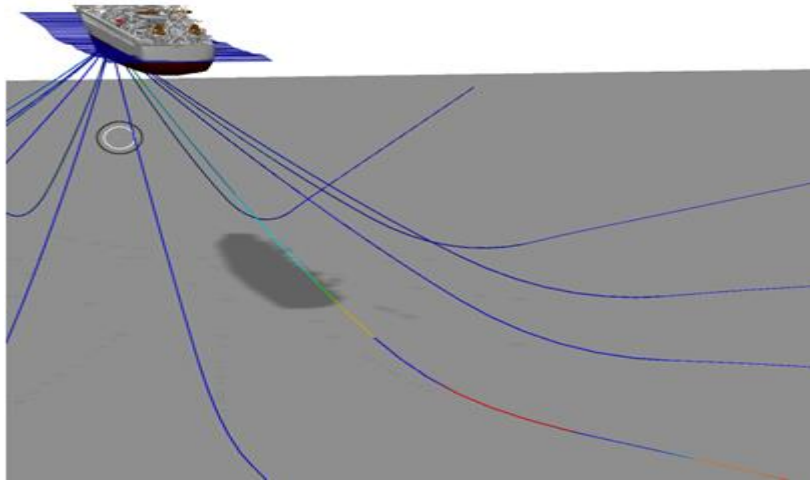


Figure 6-13 Compression pulsations (red regions) in leeward mooring

Some of the suggestions to solve this problem are as follows (Levold, 2013):

- a. Change the pretension and anchor position
- b. Increase the number of elements in the mooring lines. Between 5m and 7 m long elements should be fine. Longer elements can be used for the part that's located on the seabed.
- c. Weaken the sea bed contact parameters like stiffness and friction e.g. reduce the seabed stiffness.
- d. Reduce the time step in dynamic calculation

Looking more into the output files it was found that after some iteration gives the error message “Too large incremental rotations”. According to section 4.6.3 (RIFLEX, 2013) this error message in most case caused by use of too large incremental load steps, but can also occur by physical instability problems. So, the load step is reduced to 0.05s and the simulation was done successfully without any error. But another problem was raised which is illustrated in Figure 6-14. In this figure we can see that the tension becomes zero in some certain points and after 1500s of simulation the tension series just become crazy giving unrealistic results for the leeward lines.

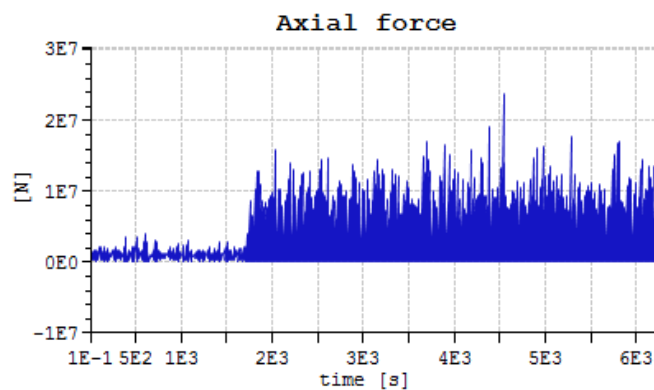


Figure 6-14 Modeling error - excessive axial force on mooring line

For our case reducing the time step even lower in dynamic calculation parameters to 0.01s has solved the problems for most of the sea states except the sea states having H_s value more than 7m and T_p value more than 12s. Finally after trying several simulations with different alternative options from the suggestions above it was found that if the axial bottom friction is not included in the simulation, the problem is solved for higher sea states also. In Figure 6-15 Time series of tension process of leeward line for sea state $H_s = 16\text{m}$ and $T_p = 18.2\text{s}$ is given and we can see that model run successfully even though the tension goes to zero at several points during the 3 hour simulation.

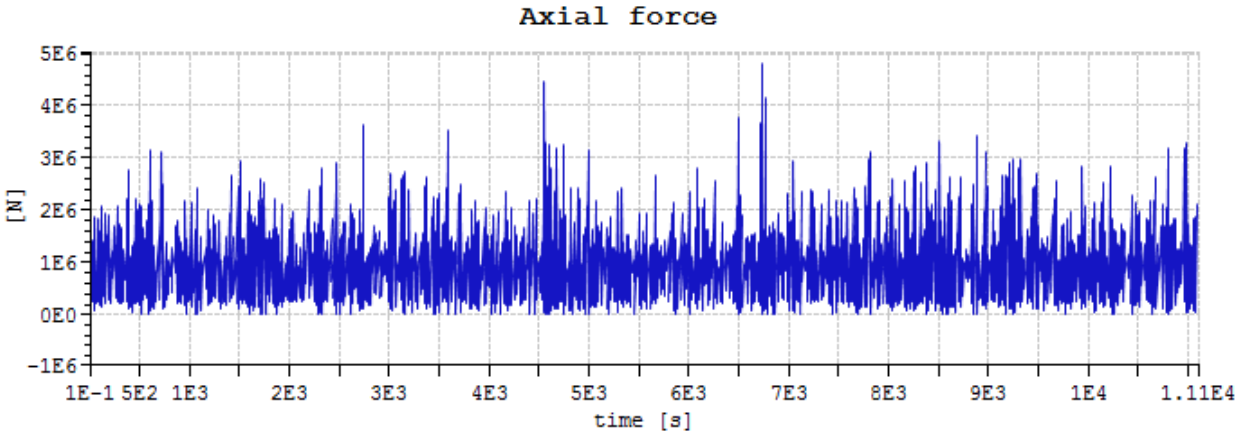


Figure 6-15 Time series of tension process for sea state $H_s = 16\text{m}$ and $T_p = 18.2\text{s}$

7 Post-processing Procedure

After carrying out the long term simulation both in SIMA and MIMOSA, post processing has been done to calculate the fatigue damage. The result from MIMOSA comprises of standard deviation (σ) and mean-up-crossing period (T_z) of the tension process for all mooring lines for each sea states. It is not straightforward to calculate fatigue damage for this type of result. One needs to use the methods described in section 5.1 earlier.

In SIMA it is possible to separate post processing task for calculating fatigue damage as shown in the following figure.

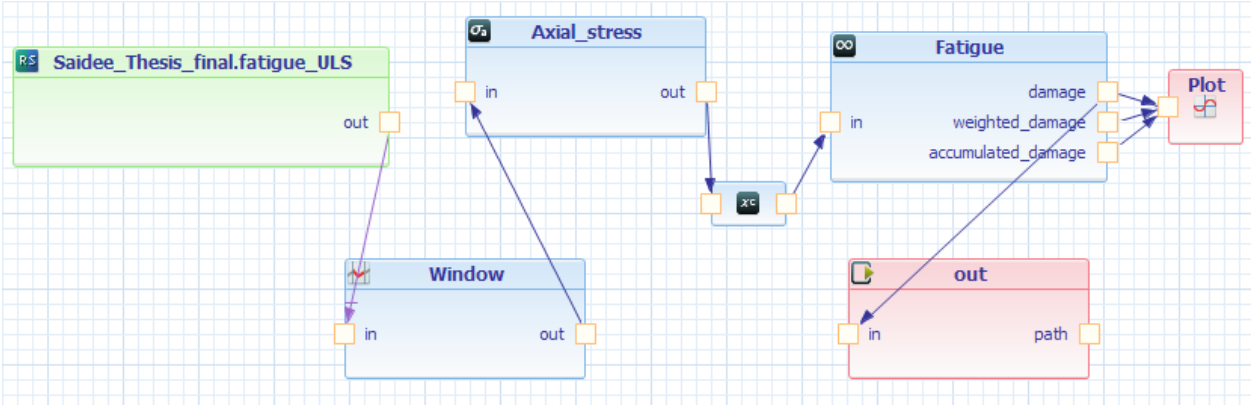


Figure 7-1 SIMA post-processing tool for fatigue damage calculation

SIMA post-processor can produce the following results.

- a. **Damage:**
Damage for each component for each sea state
- b. **Weighted damage:**
Damage for each component for each sea state, weighted with the probability of occurrence for each sea state
- c. **Accumulated damage:**
Accumulated damage for each component, that is, the sum of the weighted damage for each component

In this thesis as the H_s and T_p values are same for all environmental direction, only the result from “Damage” slot of SIMA is used to save computational time and then multiplied by the combined scatter diagram and directional probability to get the fatigue damage for each sea states. Following equation is used for this purpose. After that damage from all sea states are summed up to get the total damage for each line.

$$d_i = d_{i,3-h} \cdot P_{SC} \cdot P_{Dir} \tag{7-1}$$

Where, d_i is the calculated damage for sea state i, $d_{i,3-h}$ is damage from 3 hour simulation of SIMA, P_{SC} is scatter diagram probability, and P_{Dir} is probability of direction.

8 Results and Discussions

In this thesis mainly Tension-tension (T-T) fatigue are dealt with which is caused by the fluctuating line tension due to irregular vessel movements with low frequency and wave frequency contributions. Other types of fatigue damage are typically of the following (ISO 19901-7, 2013).

- a. Combined bending and tension (B-T) fatigue:
It mainly occurs at locations such as fairleads, bending shoes, chain stoppers, hawser pipes, bend limiting devices and adjacent to clump weights and mid-water buoys.
- b. Free bending fatigue can occur at wire rope terminations
- c. Wear and tear, deformation of chain links and wire cross sections which may occur near seabed and fairleads.
- d. Corrosion fatigue

8.1 Comparison between MIMOSA (FD analysis) and SIMA (TD analysis)

Comparison between the TD and FD has been done previously and comparison between calculation methods of MIMOSA and SIMA is given in (Chrolenko, 2013).

According to section 5.4 we know that the standard deviation of the tension process (σ_T) and the mean-up-crossing period (t_z) are the parameters that will be responsible for the differences in results. In this thesis we will look more into σ_T which is more important as it is raised to the power of m and the fatigue damage ratio will also vary significantly due to different values of σ_T .

The comparative study here is between a simplified computation method in the FD and a fully non-linear coupled analysis in TD that needs more computation time in contrast with the earlier one. For calculation of WF motion in MIMOSA dynamic model named 'ELEMENT METHOD' is used which calculates the dynamic effects in a simplified way whereas in coupled TD analysis of SIMA dynamic effects and updated line characteristics are properly accounted for. Dynamics effects mentioned here means that the drag and inertia forces on the mooring lines are included and accounted for in the computation method.

For the sea states of $H_s = 9\text{ m}$ and $T_p = 14\text{ s}$ we get the values in the following table for standard deviation of tension process and the tension values on top of mooring line for the same sea state is given in Table 8-2. Maximum tension from SIMA is calculated using one seed value only.

Table 8-1 Standard deviation of tension process

Standard deviation (σ_T)	Line 1			Line 7		
	MIMOSA	SIMA	Deviation	MIMOSA	SIMA	Deviation
σ_{T-WF} (kN)	153.57	52.7	65.68 %	221.19	75	66.09 %
σ_{T-LF} (kN)	196.3	223	-13.60 %	95.8	199	-107.72 %
$\sigma_{T-total}$ (kN)	249.2	260	-4.33 %	241	246	-2.07 %

Table 8-2 Tension values on top of mooring line calculated by MIMOSA and SIMA

MIMOSA	Line nb.	T-static (kN)	T-WF-base (kN)	T-WF (kN)	T-max (kN)
	Line 1	1942.7	2579	1376	3976
	Line 7	1184	1385	1989	3374
SIMA		T-static (kN)	T-mean (kN)	T-WF (kN)	T-max (kN)
	Line 1	1919	2017	448	3795
	Line 7	1091	1025	1343	2410

*here ‘T’ stands for tension

In order to separate the LF and WF in SIMA low pass and high pass filter is used with a cut of frequency of 0.03 Hertz. In case high pass filtered plot is quite good but in the low pass filtered plot some of high frequency component is present meaning the result might not be totally correct.

From Table 8-1 it is easily visible that σ_{WF} is very high in MIMOSA calculation than the SIMA for both line 1 and line 7 and so also the WF tension is higher in MIMOSA than SIMA Table 8-2. These differences occur due to the fact that the computation procedure of WF tension is different in MIMOSA and SIMA. WF tension in general depends on the mean offset (away from the anchor) in a progressive manner meaning the larger the mean offset (and mean tension) the larger will be the WF tension (MIMOSA, 2012).

In case of MIMOSA ‘Mean’ is the static offset along the horizontal projection of the line plus some LF offset in the same direction. It is also called as base offset. The base offset for the WF tension computation is illustrated in the Figure 8-1 where we can see that WF base offset is higher than the mean offset meaning the line will be more tensioned when calculating the WF tension and calculated WF tension will be larger. But in case of SIMA WF tension is calculated based on mean offset where the line is less tensioned and gives lower WF tension comparing to MIMOSA.

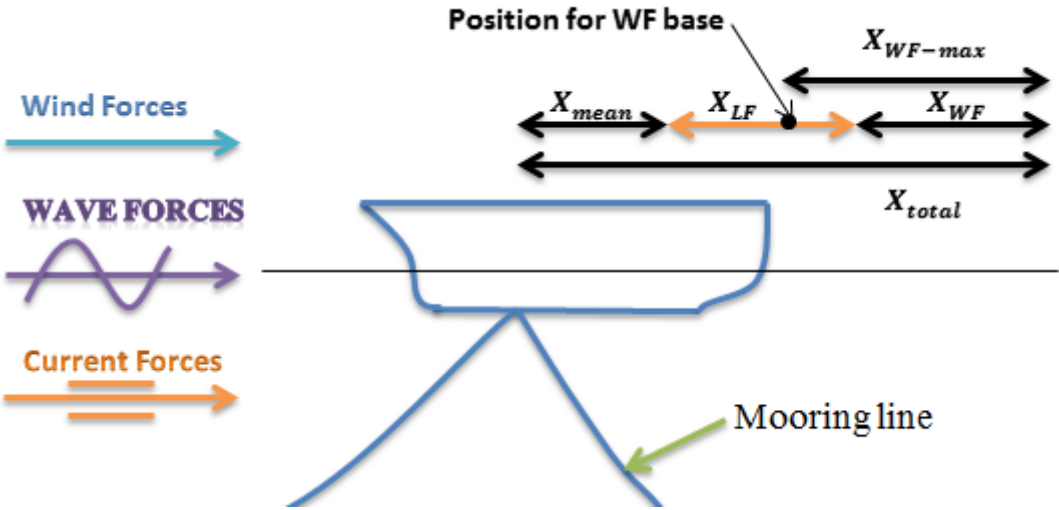


Figure 8-1 Offset for wave frequency tension calculation in MIMOSA

But when comparing results for windward and leeward line we see that both MIMOSA and SIMA yields higher values for leeward line which is reasonable as vessel is ship-shaped FPSO. More about the windward and leeward side effect will be discussed in section 8.3 later.

Even though SIMA gives lower value for σ_{T-WF} than MIMOSA the total standard deviation of the tension process $\sigma_{T-total}$ is higher in SIMA meaning that SIMA will give higher damage than MIMOSA as the ratio of σ_T is higher (eqn. [5-20]).

8.2 Comparative study between fatigue calculation methods

According to section 6.3.2 (ISO 19901-7, 2013) simple summation method will give an acceptable estimate of fatigue life if the ratio of standard deviation tensions between wave frequency and low frequency response satisfies the following condition.

$$\sigma_{WF}/\sigma_{LF} \geq 1.5 \text{ or } \sigma_{WF}/\sigma_{LF} \leq 0.05 \quad [8-1]$$

However this method may underestimate the fatigue damage if both the wave frequency and low frequency components have significant contribution. From MIMOSA for sea state of $H_s = 9m$ and $T_p = 14s$, it is found that $\sigma_{WF} = 221.4 kN$ and $\sigma_{LF} = 96.77 kN$ giving ratio, $\sigma_{WF}/\sigma_{LF} = 2.31$ which satisfies equation [7-1] and from Figure 8-2 it is evident that WF components have more effect than the LF components. So, SS method is supposed to give acceptable estimate of fatigue life.

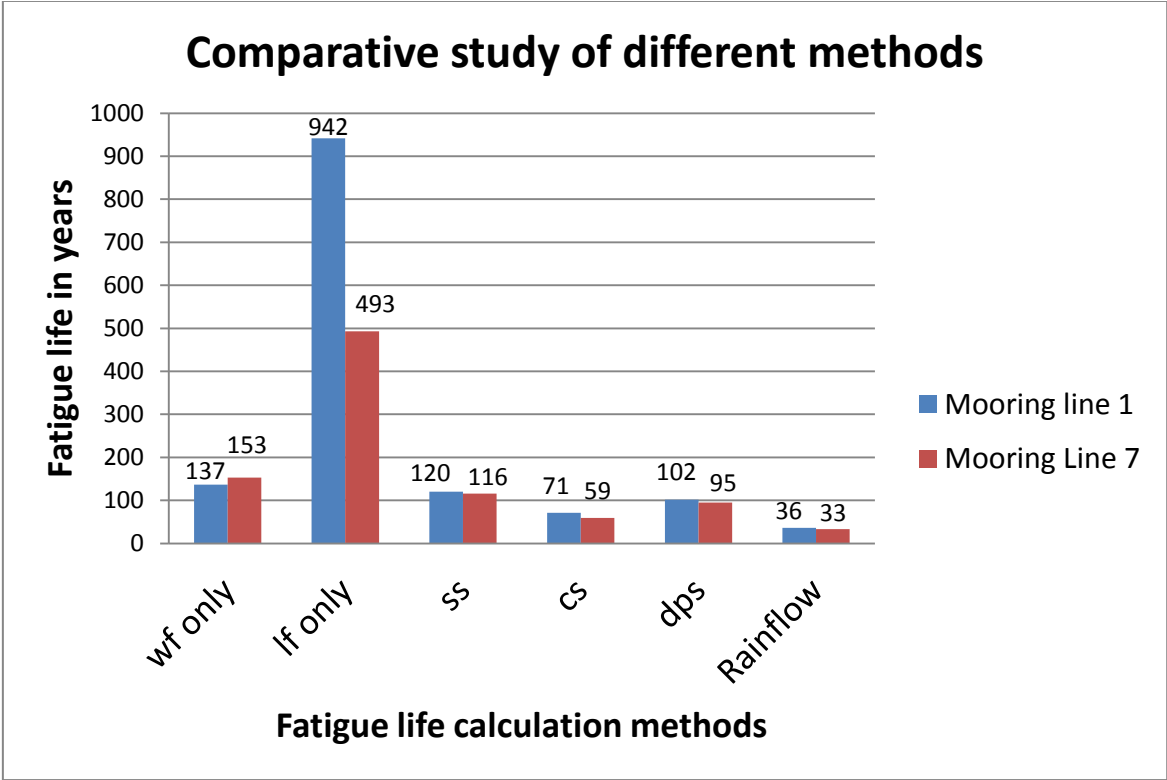


Figure 8-2 Comparative study of different fatigue analysis method

DNB approach is considered to be the most accurate method and yield less conservative results than CS approach (ISO 19901-7, 2013). It is especially suitable when WF and LF cause significant fatigue damage but if the LF content is dominant then it will overestimate the result.

Figure 8-2 illustrates the total fatigue life in years for mooring line 1 and 7 based on damaged per year from all sea states in all directions. In this figure one can see that the result from SS and DNB method are quite close and the CS method over estimates the fatigue damage. In contrast with DNB approach, damage calculated by the CS approach is 30% and 37% higher respectively for line 1 and line 7 and the damage calculated by the SS approach is 17% and 22% lower.

Damage from the TD analysis calculated by RFC is 3 times higher than DNB approach damage and twice the damage of CS approach. So, the study shows RFC will predict higher fatigue damage.

Similar comparison study has been done in (Lie & Fylling, 1994) where it was found that DNB methods with a wave frequency bandwidth parameter of 0.1 compare well with rain flow counting results while SS underestimates and CS overestimates the results. Our study yields the same result except the damage from TD analysis is much higher.

8.3 Fatigue damage of windward and leeward line

For all direction of the environmental loading, the fatigue damage of windward and leeward line based on DNB approach is given in Table 8-3.

Table 8-3 Fatigue damage of windward and leeward line for all direction

Direction (degree)	Directional Probability	Windward Line damage	Leeward Line damage
0	0.156	1.79E-03	2.53E-03
30	0.075	8.61E-04	1.22E-03
60	0.021	2.41E-04	3.41E-04
90	0.025	2.87E-04	4.06E-04
120	0.02	2.30E-04	3.24E-04
150	0.009	1.03E-04	1.46E-04
180	0.015	1.72E-04	2.43E-04
210	0.111	1.27E-03	1.80E-03
240	0.224	2.57E-03	3.63E-03
270	0.127	1.46E-03	2.06E-03
300	0.094	1.08E-03	1.53E-03
330	0.123	1.41E-03	2.00E-03

Table 8-3 shows there is a significant difference in the fatigue damage of windward and leeward line for all environmental direction. It is associated with the leeward and windward side effect which is a special type of phenomenon for ship-shaped units as shown in Figure 8-3 (Typical figure and not as scaled). In our case line number 1 is in windward side and line

number 7 is in leeward side for 0 degree environmental direction and it changes as the direction of environmental load changes.

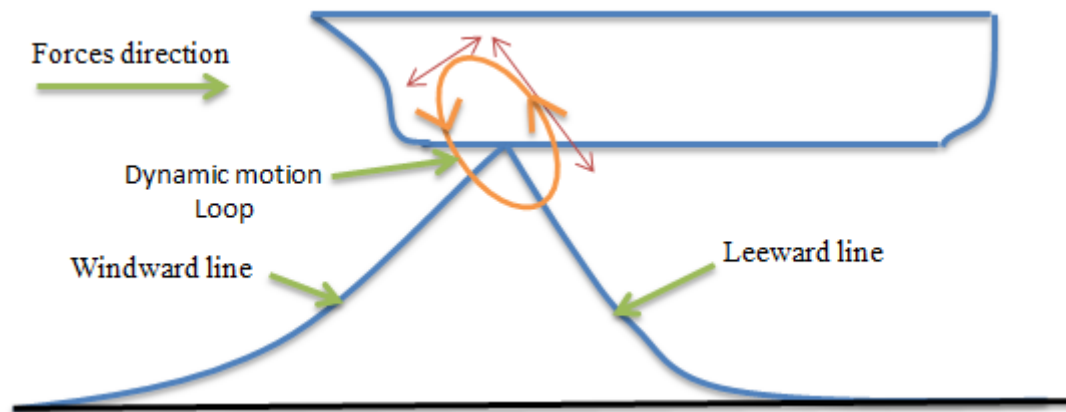


Figure 8-3 Dynamic effect on leeward and windward mooring line

In Figure 8-3 we can see that windward line is more tensioned than the leeward line. The dynamic motion follows elliptical loop and indicates the maximum displacement of both lines in their respective direction (shown by arrow). As the leeward line is more slacked the displacement is higher for it and due to this leeward side line gets higher dynamic wave motion effect even though it has less WF base tension than the windward line. This means leeward line will get higher tension contribution from wave frequency motion. The higher value of the WF tensions in leeward line will increase the fatigue damage significantly.

8.4 Effect of directional probability on fatigue damage

The directional probability of sea states is not same for all directions as given in Table 6-3. Due to the assumption that H_s and T_p values are same for all environmental direction we will not see that much variation in results for the different direction of environmental loads.

An important observation is that differences in calculated fatigue damage are more prominent in the sea states having higher probability and the higher damages are occurred for environment loads from 240 degree which has the highest directional probability (Figure 8-4) of sea states with value of 0.224. The 2nd highest is for 0 degree having probability value of 0.156 and the mooring lines also get higher damage for this sea states comparing to others.

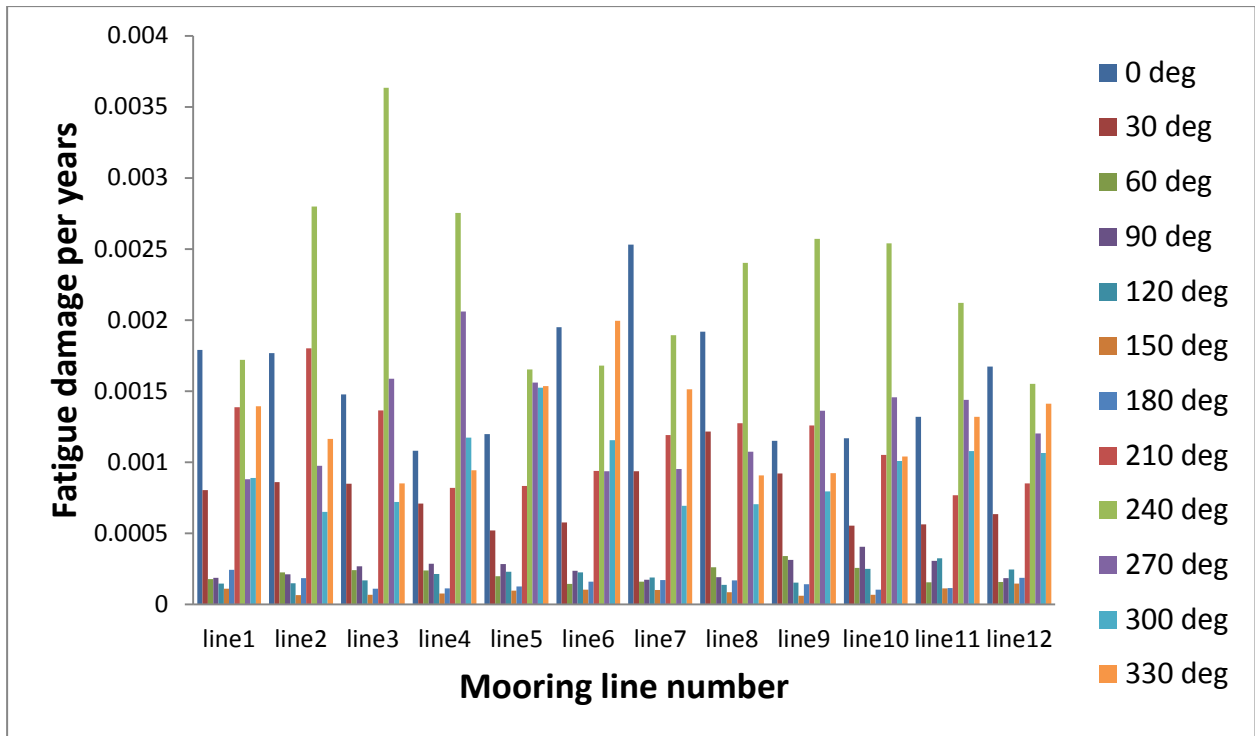


Figure 8-4 Fatigue damage for all lines in all direction using DNB approach

The highest damage is experienced by line no. 3 as shown in the above figure for environment propagating in 240 degree and it is due to the fact that it gets the highest directional probability meaning experiencing more waves and also leeward side effect as discussed in section 8.3 of this chapter.

8.5 Important sea states for fatigue damage

One of the main objectives of this thesis is to find the important sea states for the fatigue damage of mooring lines.

The scatter diagram probability of each sea state condition is plotted in Figure 8-5. It is noticeable that most of the occurrence is below H_s value of 5m and T_p value of 13s which are basically low sea states. The probability of occurrence for high sea states with higher H_s and T_p value is below 0.03.

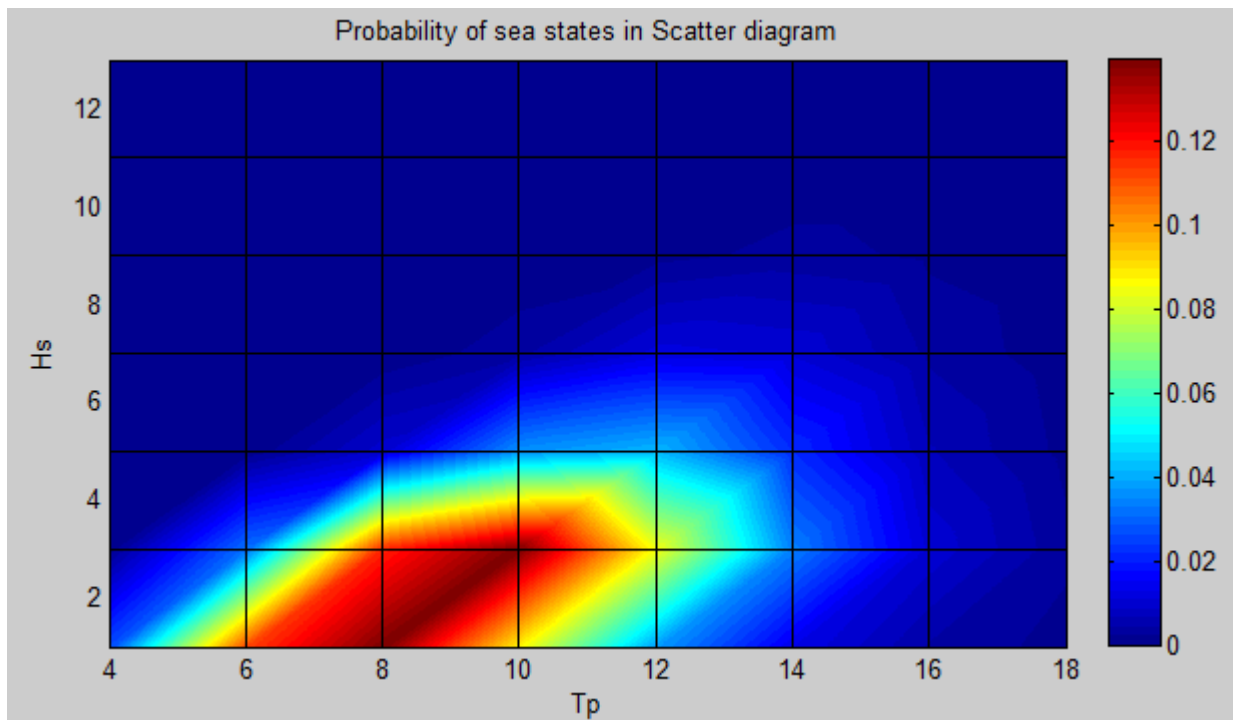


Figure 8-5 Scatter diagram probability of sea states

The fatigue damage of the mooring are also plotted in similar manner as probability of sea states to investigate the comparative damage between sea states.

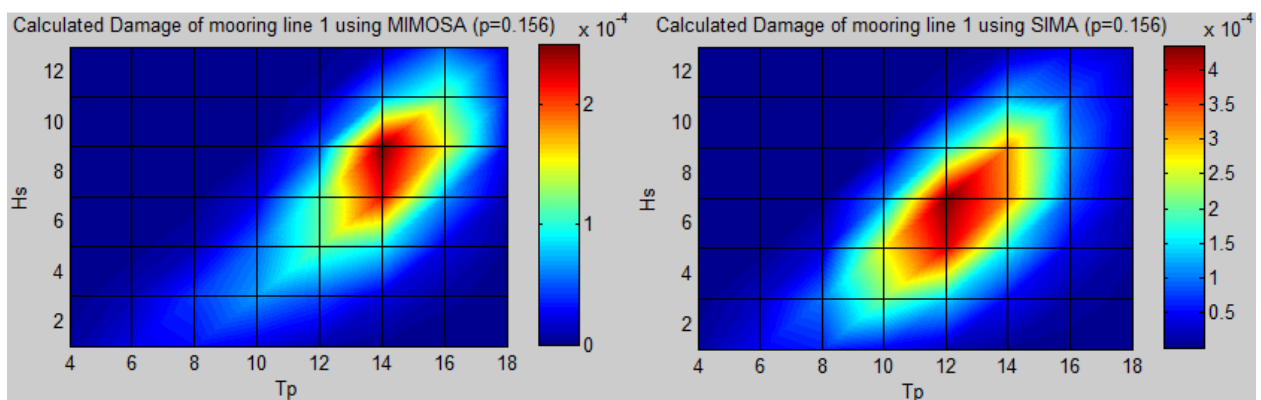


Figure 8-6 Fatigue damage calculated by MIMOSA (left) and SIMA (right) for line 1

Figure 8-6 illustrates the fatigue damage of mooring line 1 calculated by both MIMOSA and SIMA for each sea states with a specific directional probability. It is evident that for MIMOSA higher damage is found in between H_s value of 6m~10m and T_p value of 13s~16s whereas SIMA gives higher damage in between H_s value of 4m~10m and T_p value of 11s~15s. For both cases the damage is higher in higher sea states even though the occurrence is higher in low sea states according to Figure 8-5.

Another important observation is that SIMA predicts more damage for wide range of H_s and T_p values than MIMOSA and the highest damage is found in SIMA for $H_s = 7\text{m}$ and $T_p = 12\text{s}$ while the highest damage in MIMOSA is found for $H_s = 9\text{m}$ and $T_p = 14\text{s}$.

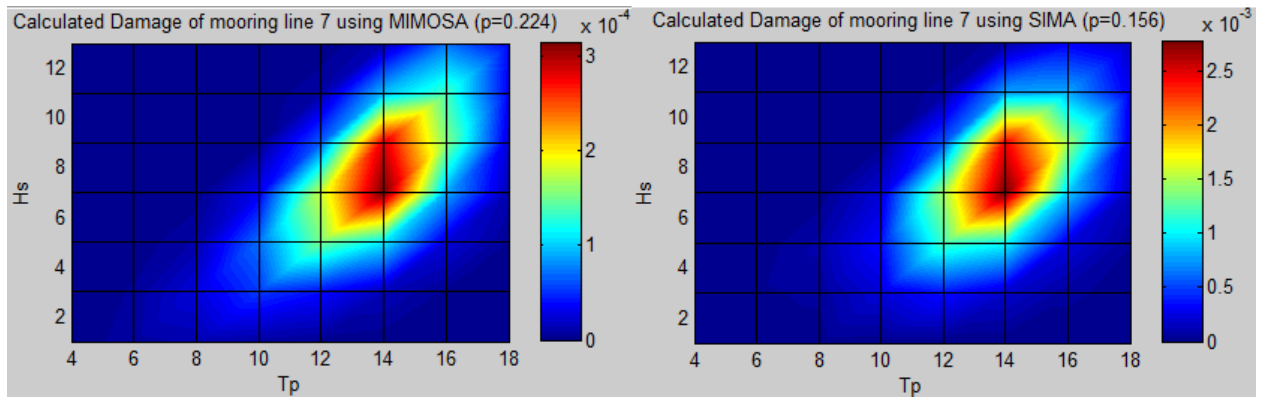


Figure 8-7 Fatigue damage calculated by MIMOSA (left) and SIMA (right) for line 7

In case of mooring line 7 results from MIMOSA and SIMA corresponds to each other very well. Both software predicts higher damage in almost the same sea states (between H_s value of 6m~10m and T_p value of 12s~15s).

8.6 Simplified method for estimating fatigue damage (FLS) from the ULS results

Our intension is to examine the possibility to estimate fatigue damage by using information from the ULS design results together with a simplified method using the long term distribution of line tensions. The reason behind the intension is that regulations require calculations for fatigue damage only for permanent floating units, e.g. FPSO and FSO. Section 8.1.2.5 (ISO 19901-7, 2013) states that fatigue analysis is not required for MODUs. But it is worth discussing if fatigue analysis should be required for mobile units.

A report on mooring line failures (Kvitrud, 2014) shows that three of fatigue failures occurred in Norwegian continental shelf during 2010 to 2014 were on MODUs. So, it is better to design the MODUs based on FLS criteria, but detailed fatigue analysis are claimed to be unrealistic for site specific evaluations of MODUs as they operates in different locations. Therefore, we have tried to propose a simplified method to estimate the fatigue damage using the results we already have from ULS calculations.

Using the closed form solution as described in section 5.2.1 based on Weibull equation [5-13] for fatigue calculation. The equation is stated again below.

$$\text{Fatigue damage, } D = \frac{n_0}{a_D} \cdot \frac{\Delta\sigma_0^m}{(\ln n_0)^{\frac{m}{h}}} \cdot \Gamma\left(\frac{m}{h} + 1\right)$$

If we can find the $\Delta\sigma_0$ and n_0 from ULS conditions and the Weibull parameter is known we can calculate the fatigue damage using the above equation. But the Weibull parameter varies from 0.5 to 1.5 and we need to find a suitable one for our case.

In order to find the correct Weibull parameter first value of $\Delta\sigma_0$ and n_0 is assumed. $\Delta\sigma_0$ is calculated by the equation below.

$$\Delta\sigma_0 = \frac{\Delta T}{A} \quad [8-2]$$

Where ΔT is assumed by the following equation and A is the nominal cross-sectional area of the mooring line component as given in chapter 5.

$$\Delta T = (T_{MPM} - T_{mean}) \cdot 2 \quad [8-3]$$

Here, T_{MPM} is the most probable largest maximum tension for ULS design condition and T_{mean} is the mean value of tension process for ULS design condition.

The number of cycles is assumed to be equal to the number of cycles of ULS design condition calculated by DNB approach from MIMOSA long term simulation result using the following equation.

$$n_0 = v_p \cdot T_{1-year} \quad [8-4]$$

Here, v_p is the mean up-crossing rate of the same sea state from which tension values are calculated. In our case it is the ULS sea state. v_p can be calculated using equation [5-11] and T_{1-year} is total time in second for one year.

After doing the calculation by using above equations for ULS sea state ($H_s = 16\text{m}$ and $T_p = 18.2\text{s}$) we get the values given in the following table.

Table 8-4 Results from ULS design condition ($H_s = 16\text{m}$ and $T_p = 18.2\text{s}$)

Line nb.	T_{MPM} (MN)	T_{mean} (MN)	ΔT (MN)	$\Delta\sigma_0$ (MPa)	n_0
Line 1	7.2428	2.1164	10.2528	10.2528	163121
Line 7	7.1875	1.1042	12.1666	12.1666	61958

For the fatigue damage, the damage calculated by the Rain flow counting method is considered as it supposed to give relatively accurate results and same S-N curve is used as in RFC method for values of m and a_D . Now as we know all the values parameter, h can be found solving equation [5-13]. The nonlinear equation is solved using MATHCAD software. Script for solving the equation is given in APPENDIX E.

Finally we get the values of parameter h for the corresponding damage of line 1 and line 7 given in Table 8-5 and the values are within the range of 0.5 to 1.5 which is acceptable as shown in Figure 5-3.

Table 8-5 Approximate values of Weibull parameter, h

Line number	Damage per year	Calculated value of 'h'
Line 1	0.0275	0.559
Line 7	0.0301	0.575

Approximate shape of the long term stress distribution is given in the following figure based on the calculated Weibull parameter above. The figure is only for illustration to show how the long term stress will be distributed.

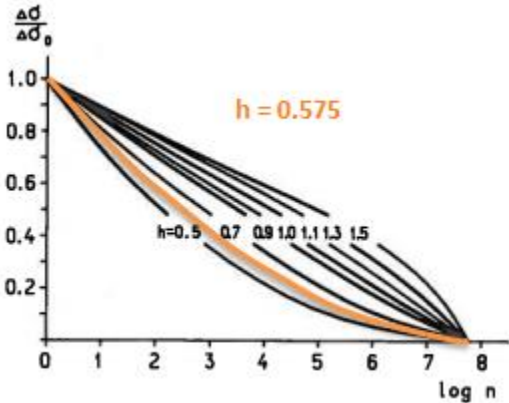


Figure 8-8 Approximate shape of long term stress distribution

Using the Weibull parameter, h given in Table 8-5 it is now possible to estimate the approximate fatigue damage of mooring line by using equation [5-13] based on the results ($\Delta\sigma_0$ and n_0 values) from ULS design condition.

In the North Sea environment, the inertia dominated response gives h-values in the range of 1 - 1.5 and Drag dominated response gives h-values in the range 0.7 – 1.3 (Lie, 1992). In our case the h-values are slightly lower than the 2nd range. Drag forces on the mooring line are believed to be the most significant non-linear effect on the dynamic tension amplitude. Therefore, further work should be done in order to obtain more information of h-values.

9 Conclusion

9.1 Conclusion from results and discussion

Based on the result and discussion and the comparative study presented above, following conclusions are made.

- i. After comparing the TD and FD analysis it is found that even though SIMA gives lower value for wave frequency standard deviation, σ_{T-WF} than MIMOSA the total standard deviation of the tension process $\sigma_{T-total}$ is higher in SIMA meaning that TD will predict higher fatigue damage than FD analysis.
- ii. In this this thesis effort is also given to check the differences in fatigue damage between windward and leeward line. The study shows that both FD and TD results yields higher standard deviation of wave frequency tension for leeward line than windward meaning leeward line will get higher tension contribution from wave frequency motion. The higher value of the WF tensions in leeward line will increase the fatigue damage significantly.
- iii. In contrast with dual narrowband (DNB) approach, fatigue damage calculated by the combined spectrum (CS) approach is 30% and 37% higher respectively for line 1 and line 7 and the damage calculated by the SS approach is 17% and 22% lower respectively for line 1 and line 7. As the WF damage is more dominant than LF damage in our case SS approach yields very good results.
Damage from the TD analysis calculated by rain-flow counting (RFC) is 3 times higher than DNB approach damage and twice the damage of CS approach. So, the study shows RFC will predict very high fatigue damage. Therefore, it is recommended to do TD analysis to be sure about the fatigue damage. Otherwise only doing FD analysis one might under predicts the fatigue damage leading to failure of the mooring lines in future due to fatigue.
- iv. An important observation is that calculated fatigue damage are more prominent in the sea states having higher directional probability meaning experiencing more waves and also leeward side effect is higher provided that H_s and T_p values are same for all environmental direction.
- v. For both cases the damage is higher in higher sea states even though the occurrence level is higher in low sea states. It is evident from MIMOSA results that higher damages occur in between H_s value of 6m~10m and T_p value of 13s~16s whereas SIMA results give higher damage in between H_s value of 4m~10m and T_p value of 11s~15s. In both cases sea states with H_s more than 11m and less than 3m give very low fatigue damage, therefore, can be neglected in cage of fatigue damage calculation.
- vi. A study is also conducted to examine the possibility to estimate fatigue damage by using information from the ULS design results together with a simplified method using the long term distribution of line tensions. It is found that using the Weibull parameter, h given in the Table 8-5 it might be possible to estimate the approximate fatigue damage of mooring line by using equation [5-13] based on the results from ULS design condition.

9.2 Recommendation for future work

Following are some recommendation for future work in connection with this thesis.

- a. In this thesis modeling is done for 320 m water depth. But nowadays mooring systems are designed for deep seas where mooring lines have higher pretensions than shallow water. So, in future it is recommended to check fatigue life for deep sea mooring system.
- b. An assumption of this thesis is that H_s and T_p values are same for all environmental direction we will not see that much variation in results for the different direction of environmental loads. Use of H_s and T_p varying with direction can be used for future work to see the effect of this.
- c. As we have seen in this thesis high sea states gives higher damage to fatigue, it will be worth checking weather introducing thrusters can reduce the fatigue damage in those sea states.
- d. The Weibull parameter, h from simplified method (section 8.6) is calculated for FPSO and for 320 m water depth. In future one can check if the value of h changes in case of semi-submersible and deep seas.

10 Bibliography

- Almar-Næss. (1985). *Fatigue Handbook: offshore steel structures, Chapter 10: Fatigue life calculation*.
- API. (2005). *API Recommended practice 2SK, Design and analysis of station keeping systems for floating structures*.
- Berge, S. (2006). *Fatigue and fracture design of marine structures II (compendium for course TMR 4200)*.
- Chrolenko, M. O. (2013). *Dynamic Analysis and Design of Mooring Lines*. Trondheim: NTNU.
- DNV. (2013). *DNV offshore standard, DNV-OS-E301 Position Mooring*. Norway: DNV.
- Faltinsen, O. M. (1990). *Sea loads on ships and offshore structures*. Cambridge University Press.
- ISO 19901-7. (2013). *Part 7: Stationkeeping systems for floating offshore structures and mobile offshore units*.
- Kvitrud, A. (2014). *Anchor line failure- Norwegian Continental Shelf- 2010-2014*.
- Larsen, C. M. (2012). *Marine dynamics; compendium for course TMR 4182 Marine dynamics*.
- Larsen, K. (2014). Lecture note on Mooring and station keeping of floating structures (TMR4500 specialization project).
- Larsen, K., & Ormberg, H. (1998). Coupled analysis of floater motion and mooring dynamics for a turret-moored ship. *Applied Ocean Research*, 55-67.
- Levold, P. (2013). Private communication. Trondheim.
- Lie, H. (1992). Simplified fatigue analysis of mooring lines. *Posisjoneringmøtet '92; 7.-9. oktober, Fagernes*.
- Lie, H., & Fylling, I. (1994). Evaluation of methods for fatigue analysis of offshore mooring lines. *Offshore South East Asia 10th Conference & Exhibition*. Singapore.
- MIMOSA. (2012). *MIMOSA User's Documentation, Program version 6.3-06*. MARINTEK.
- Ramnäs. (2014, December). Retrieved from <http://ramnas.com/>: <http://ramnas.com/wp-content/uploads/2012/11/Ramnas-Technical-Broschure.pdf>
- RIFLEX. (2013). *RIFLEX theory manual V4.0rev3*. Trondheim: MARINTEK.
- Saidee, M. H. (2014). *Parameters Sensitivity on Mooring Loads of Ship-Shaped FPSOs*. Trondheim.

SIMO. (2012). *SIMO - theory manual version 4.0 rev. 1*. MARINTEK.

Statoil. (2004). *Heidrun Metocean Design Basis*.

Vryh of Anchors BV. (2010). Retrieved from http://www.vryhof.com/anchor_manual.pdf

APPENDIX A

Information Retrieval

In order to ensure good quality of the product it is mandatory to use data and information from reliable source. In this chapter a short description will be given how the information is retrieved for this master thesis.

For this thesis the lecture notes provided by the supervisor during the project work is used for many cases. Some of the related books and papers are also provided by him specially “Fatigue Hand Book”.

Compendium for different courses throughout the whole Master program in NTNU were of great help for this thesis and used when ever needed. The library of the department and NTNU University online library is used to find relevant literature.

Theory manual of the software from MARINTEK is used for describing some of the theory part of the thesis.

Apart from this Google search engine is also used to find information on general topics whenever needed.

APPENDIX B

Program list

Program Name	Version	Function
MIMOSA	6.3-06	MARINTEK program: Frequency domain analysis
SIMA	3.1.1.12020	MARINTEK program: Coupled time domain analysis using (SIMO & RIFLEX)
Excel	10	Post-processing result and data plotting
MATLAB	R2013a	Mainly for data Plotting
MATHCAD	15 (Trial)	Solving non-linear equation
Text Pad	7	Editor used for scripts and batch file

APPENDIX C

MIMOSA mooring file

```
*****
VESSEL POSITION
*****
'chmoor
BODY: 12 mooring lines - 1 characteristic
'x1ves x2ves x3ves x6ves
0.0000000 0.0000000 0.0000000 180.0000000
'-----
LINE DATA
'iline lichar inilin iwirun intact
1 1 1 0 1
'tpx1 tpx2
100.0000 0.0000000
'alfa tens xwinch
0 1500.000 0.0000000
'-----
LINE DATA
'iline lichar inilin iwirun intact
2 1 1 0 1
'tpx1 tpx2
100.0000 0.0000000
'alfa tens xwinch
30 1500.000 0.0000000
'-----
LINE DATA
'iline lichar inilin iwirun intact
3 1 1 0 1
'tpx1 tpx2
100.0000 0.0000000
'alfa tens xwinch
60 1500.000 0.0000000
'-----
LINE DATA
'iline lichar inilin iwirun intact
4 1 1 0 1
'tpx1 tpx2
100.000000 0.0000000
'alfa tens xwinch
90 1500.000 0.0000000
'-----
LINE DATA
'iline lichar inilin iwirun intact
5 1 1 0 1
'tpx1 tpx2
100.0000 0.0000000
'alfa tens xwinch
```

120 1500.000 0.0000000

LINE DATA

'iline lichar inilin iwirun intact

6 1 1 0 1

'tpx1 tpx2

100.0000 0.0000000

'alfa tens xwinch

150 1500.000 0.0000000

LINE DATA

'iline lichar inilin iwirun intact

7 1 1 0 1

'tpx1 tpx2

100.00000 0.0000000

'alfa tens xwinch

180 1500.000 0.0000000

LINE DATA

'iline lichar inilin iwirun intact

8 1 1 0 1

'tpx1 tpx2

100.0000 0.0000000

'alfa tens xwinch

210 1500.000 0.0000000

LINE DATA

'iline lichar inilin iwirun intact

9 1 1 0 1

'tpx1 tpx2

100.0000 0.0000000

'alfa tens xwinch

240 1500.000 0.0000000

LINE DATA

'iline lichar inilin iwirun intact

10 1 1 0 1

'tpx1 tpx2

100.0000 0.0000000

'alfa tens xwinch

270 1500.000 0.0000000

LINE DATA

'iline lichar inilin iwirun intact

11 1 1 0 1

'tpx1 tpx2

100.0000 0.0000000

'alfa tens xwinch

300 1500.000 0.0000000

```

LINE DATA
'iline lichar inilin iwirun intact
12 1 1 0 1
'tpx1 tpx2
100.0000 0.0000000
'alfa tens xwinch
330 1500.000 0.0000000
'-----
'-----
LINE CHARACTERISTICS DATA
'lichar
1
'linpty npocha npv
2 40 2
'nseg ibotco icurli
4 1 0
'anbot tpx3 x3ganc tmax fric
0.0000000 14.2000000 320.0000000 25250.0000000 0.6000000
'iseg ieltyp nel ibuoy sleng nea brkstr
1 0 30 0 930.0000000 1 16992
2 0 30 0 285.0000000 1 18033
3 0 20 0 300.0000000 1 18000
4 0 10 0 52.0000000 1 19089
'iseg dia emod emfact uwiw watfac cdn cdl
1 0.1370000 5.10500e+07 2.0000000 3.1970000 0.8700000 2.40000 0.0
2 0.1420000 5.09500e+07 2.0000000 3.4270000 0.8700000 2.4000 0.0
3 0.1470000 1.13000e+08 1.0000000 0.7872500 0.8100000 1.80000 0.0
4 0.1470000 5.08520e+07 2.0000000 3.6800000 0.8700000 2.40000 0.0
'-----
'-----
'THRUSTER DATA
'chtrus
'Thruster data information
'nthrus
'5
'ithrus ttpx1 ttpx2 tforce tdir ithrty ftmax ithrdp
'1 -128.9000000 8.0000000 0.0000000 -90.0000000 1 410.1000000 1
'2 -128.9000000 -8.0000000 0.0000000 -90.0000000 1 410.2000000 1
'3 -122.9000000 0.0000000 0.0000000 -90.0000000 1 410.3000000 1
'4 106.3000000 0.0000000 0.0000000 -90.0000000 1 410.4000000 1
'5 111.9000000 0.0000000 0.0000000 -90.0000000 1 410.5000000 1
END

```

MIMOSA macro file for long term simulation

```

READ SYSTEM 'SYSTEM
READ ENVIRONMENT FILE 'SYSTEM READ
E:\mimosa\envlongULS.txt
Double-peaked Spectrum 'SPECTRUM TYPE

```

TIME2 on ENVFIL ' PICK ONE ITEM FOR SAVING ; Return = End input
 TIME3 on ENVFIL ' PICK ONE ITEM FOR SAVING ; Return = End input
 TIME4 on ENVFIL ' PICK ONE ITEM FOR SAVING ; Return = End input
 Sign. wave height (m) ' PICK ONE ITEM FOR SAVING ; Return = End input
 Peak wave period (s) ' PICK ONE ITEM FOR SAVING ; Return = End input
 Return ' PICK ONE ITEM FOR SAVING ; Return = End input
 Return ' SYSTEM READ
 MODIFY SYSTEM ' SYSTEM
 ENVIRONMENTAL CONDITIONS ' MODIFY SYSTEM
 Wind ' DEFINE/MODIFY ENVIRONMENT
 i ' Choose type (D, H, I or A)
 / ' Mean wind speed (m/s)
 / ' Height (m)
 / ' Wind direction (deg)
 Return ' PICK ONE ITEM FOR SAVING ; Return = End input
 Return ' DEFINE/MODIFY ENVIRONMENT
 / ' Print environment data to file ? (N)
 Return ' MODIFY SYSTEM
 MOORING SYSTEM COMPUTATION ' SYSTEM
 / ' Result to file ? (N)
 Return ' PICK ONE ITEM FOR SAVING ; Return = End input
 Return ' PICK ONE ITEM FOR SAVING ; Return = End input
 EQUILIBRIUM POSITION ' MOORING SYSTEM COMPUTATIONS
 y ' Move vessel to equilibrium position? (Y)
 / ' Results to file ? (N)
 Return ' PICK ONE ITEM FOR SAVING ; Return = End input
 / ' Result to file ? (N)
 Return ' PICK ONE ITEM FOR SAVING ; Return = End input
 Return ' PICK ONE ITEM FOR SAVING ; Return = End input
 MAXIMUM LINE TENSIONS ' MOORING SYSTEM COMPUTATIONS
 ALL LINES ' SELECTION OF LINES FOR TENSION RESPONSE
 WF MOTION ' MOTION TYPE TO COMPUTE TENSION FOR
 ELEMENT METHOD ' METHOD OF TENSION CALCULATION
 / ' Write mooring tension transfer function to report file? (N)
 / ' Calculate results for each segment? (N)
 / ' Show load on anchor ? (N)
 / ' Results to file ? (N)
 a ' Line number
 Return ' PICK ONE ITEM FOR SAVING ; Return = End input
 Line001 StDev Ten WF ' PICK ONE ITEM FOR SAVING ; Return = End input
 Line001 Tz Ten WF ' PICK ONE ITEM FOR SAVING ; Return = End input
 Return ' PICK ONE ITEM FOR SAVING ; Return = End input
 Return ' PICK ONE ITEM FOR SAVING ; Return = End input
 Line002 StDev Ten WF ' PICK ONE ITEM FOR SAVING ; Return = End input
 Line002 Tz Ten WF ' PICK ONE ITEM FOR SAVING ; Return = End input
 Return ' PICK ONE ITEM FOR SAVING ; Return = End input
 Return ' PICK ONE ITEM FOR SAVING ; Return = End input
 Line003 StDev Ten WF ' PICK ONE ITEM FOR SAVING ; Return = End input
 Line003 Tz Ten WF ' PICK ONE ITEM FOR SAVING ; Return = End input
 Return ' PICK ONE ITEM FOR SAVING ; Return = End input

```

Return          ' PICK ONE ITEM FOR SAVING ; Return = End input
Line004 StDev Ten WF      ' PICK ONE ITEM FOR SAVING ; Return = End input
Line004 Tz Ten WF        ' PICK ONE ITEM FOR SAVING ; Return = End input
Return          ' PICK ONE ITEM FOR SAVING ; Return = End input
Return          ' PICK ONE ITEM FOR SAVING ; Return = End input
Line005 StDev Ten WF      ' PICK ONE ITEM FOR SAVING ; Return = End input
Line005 Tz Ten WF        ' PICK ONE ITEM FOR SAVING ; Return = End input
Return          ' PICK ONE ITEM FOR SAVING ; Return = End input
Return          ' PICK ONE ITEM FOR SAVING ; Return = End input
Line006 StDev Ten WF      ' PICK ONE ITEM FOR SAVING ; Return = End input
Line006 Tz Ten WF        ' PICK ONE ITEM FOR SAVING ; Return = End input
Return          ' PICK ONE ITEM FOR SAVING ; Return = End input
Return          ' PICK ONE ITEM FOR SAVING ; Return = End input
Line007 StDev Ten WF      ' PICK ONE ITEM FOR SAVING ; Return = End input
Line007 Tz Ten WF        ' PICK ONE ITEM FOR SAVING ; Return = End input
Return          ' PICK ONE ITEM FOR SAVING ; Return = End input
Return          ' PICK ONE ITEM FOR SAVING ; Return = End input
Line008 StDev Ten WF      ' PICK ONE ITEM FOR SAVING ; Return = End input
Line008 Tz Ten WF        ' PICK ONE ITEM FOR SAVING ; Return = End input
Return          ' PICK ONE ITEM FOR SAVING ; Return = End input
Return          ' PICK ONE ITEM FOR SAVING ; Return = End input
Line009 StDev Ten WF      ' PICK ONE ITEM FOR SAVING ; Return = End input
Line009 Tz Ten WF        ' PICK ONE ITEM FOR SAVING ; Return = End input
Return          ' PICK ONE ITEM FOR SAVING ; Return = End input
Return          ' PICK ONE ITEM FOR SAVING ; Return = End input
Line010 StDev Ten WF      ' PICK ONE ITEM FOR SAVING ; Return = End input
Line010 Tz Ten WF        ' PICK ONE ITEM FOR SAVING ; Return = End input
Return          ' PICK ONE ITEM FOR SAVING ; Return = End input
Return          ' PICK ONE ITEM FOR SAVING ; Return = End input
Line011 StDev Ten WF      ' PICK ONE ITEM FOR SAVING ; Return = End input
Line011 Tz Ten WF        ' PICK ONE ITEM FOR SAVING ; Return = End input
Return          ' PICK ONE ITEM FOR SAVING ; Return = End input
Return          ' PICK ONE ITEM FOR SAVING ; Return = End input
Line012 StDev Ten WF      ' PICK ONE ITEM FOR SAVING ; Return = End input
Line012 Tz Ten WF        ' PICK ONE ITEM FOR SAVING ; Return = End input
Return          ' PICK ONE ITEM FOR SAVING ; Return = End input
Return          ' PICK ONE ITEM FOR SAVING ; Return = End input
/              ' Plot on screen ? (N)
/              ' Plot to file ? (N)
MAXIMUM LINE TENSIONS      ' MOORING SYSTEM COMPUTATIONS
ALL LINES                ' SELECTION OF LINES FOR TENSION RESPONSE
LF MOTION                 ' MOTION TYPE TO COMPUTE TENSION FOR
/              ' Calculate results for each segment? (N)
/              ' Show load on anchor ? (N)
/              ' Results to file ? (N)
a                          ' Line number
Return          ' PICK ONE ITEM FOR SAVING ; Return = End input
Line001 StDev Ten LF      ' PICK ONE ITEM FOR SAVING ; Return = End input
Line001 Tz Ten LF        ' PICK ONE ITEM FOR SAVING ; Return = End input
Return          ' PICK ONE ITEM FOR SAVING ; Return = End input

```

```

Return          ' PICK ONE ITEM FOR SAVING ; Return = End input
Line002 StDev Ten LF      ' PICK ONE ITEM FOR SAVING ; Return = End input
Line002 Tz Ten LF        ' PICK ONE ITEM FOR SAVING ; Return = End input
Return          ' PICK ONE ITEM FOR SAVING ; Return = End input
Return          ' PICK ONE ITEM FOR SAVING ; Return = End input
Line003 StDev Ten LF      ' PICK ONE ITEM FOR SAVING ; Return = End input
Line003 Tz Ten LF        ' PICK ONE ITEM FOR SAVING ; Return = End input
Return          ' PICK ONE ITEM FOR SAVING ; Return = End input
Return          ' PICK ONE ITEM FOR SAVING ; Return = End input
Line004 StDev Ten LF      ' PICK ONE ITEM FOR SAVING ; Return = End input
Line004 Tz Ten LF        ' PICK ONE ITEM FOR SAVING ; Return = End input
Return          ' PICK ONE ITEM FOR SAVING ; Return = End input
Return          ' PICK ONE ITEM FOR SAVING ; Return = End input
Line005 StDev Ten LF      ' PICK ONE ITEM FOR SAVING ; Return = End input
Line005 Tz Ten LF        ' PICK ONE ITEM FOR SAVING ; Return = End input
Return          ' PICK ONE ITEM FOR SAVING ; Return = End input
Return          ' PICK ONE ITEM FOR SAVING ; Return = End input
Line006 StDev Ten LF      ' PICK ONE ITEM FOR SAVING ; Return = End input
Line006 Tz Ten LF        ' PICK ONE ITEM FOR SAVING ; Return = End input
Return          ' PICK ONE ITEM FOR SAVING ; Return = End input
Return          ' PICK ONE ITEM FOR SAVING ; Return = End input
Line007 StDev Ten LF      ' PICK ONE ITEM FOR SAVING ; Return = End input
Line007 Tz Ten LF        ' PICK ONE ITEM FOR SAVING ; Return = End input
Return          ' PICK ONE ITEM FOR SAVING ; Return = End input
Return          ' PICK ONE ITEM FOR SAVING ; Return = End input
Line008 StDev Ten LF      ' PICK ONE ITEM FOR SAVING ; Return = End input
Line008 Tz Ten LF        ' PICK ONE ITEM FOR SAVING ; Return = End input
Return          ' PICK ONE ITEM FOR SAVING ; Return = End input
Return          ' PICK ONE ITEM FOR SAVING ; Return = End input
Line009 StDev Ten LF      ' PICK ONE ITEM FOR SAVING ; Return = End input
Line009 Tz Ten LF        ' PICK ONE ITEM FOR SAVING ; Return = End input
Return          ' PICK ONE ITEM FOR SAVING ; Return = End input
Return          ' PICK ONE ITEM FOR SAVING ; Return = End input
Line010 StDev Ten LF      ' PICK ONE ITEM FOR SAVING ; Return = End input
Line010 Tz Ten LF        ' PICK ONE ITEM FOR SAVING ; Return = End input
Return          ' PICK ONE ITEM FOR SAVING ; Return = End input
Return          ' PICK ONE ITEM FOR SAVING ; Return = End input
Line011 StDev Ten LF      ' PICK ONE ITEM FOR SAVING ; Return = End input
Line011 Tz Ten LF        ' PICK ONE ITEM FOR SAVING ; Return = End input
Return          ' PICK ONE ITEM FOR SAVING ; Return = End input
Return          ' PICK ONE ITEM FOR SAVING ; Return = End input
Line012 StDev Ten LF      ' PICK ONE ITEM FOR SAVING ; Return = End input
Line012 Tz Ten LF        ' PICK ONE ITEM FOR SAVING ; Return = End input
Return          ' PICK ONE ITEM FOR SAVING ; Return = End input
Return          ' PICK ONE ITEM FOR SAVING ; Return = End input
/                  ' Plot on screen ? (N)
/                  ' Plot to file ? (N)
SYSTEM            ' MOORING SYSTEM COMPUTATIONS
READ SYSTEM       ' SYSTEM
WRITE RESPONSE FILE ' SYSTEM READ

```

```
longterm.results      ' Response file
53                    ' Values per record
/
Return                ' SYSTEM READ
@ CLOSE
```

APPENDIX D

All plots for vessel hydrodynamic properties

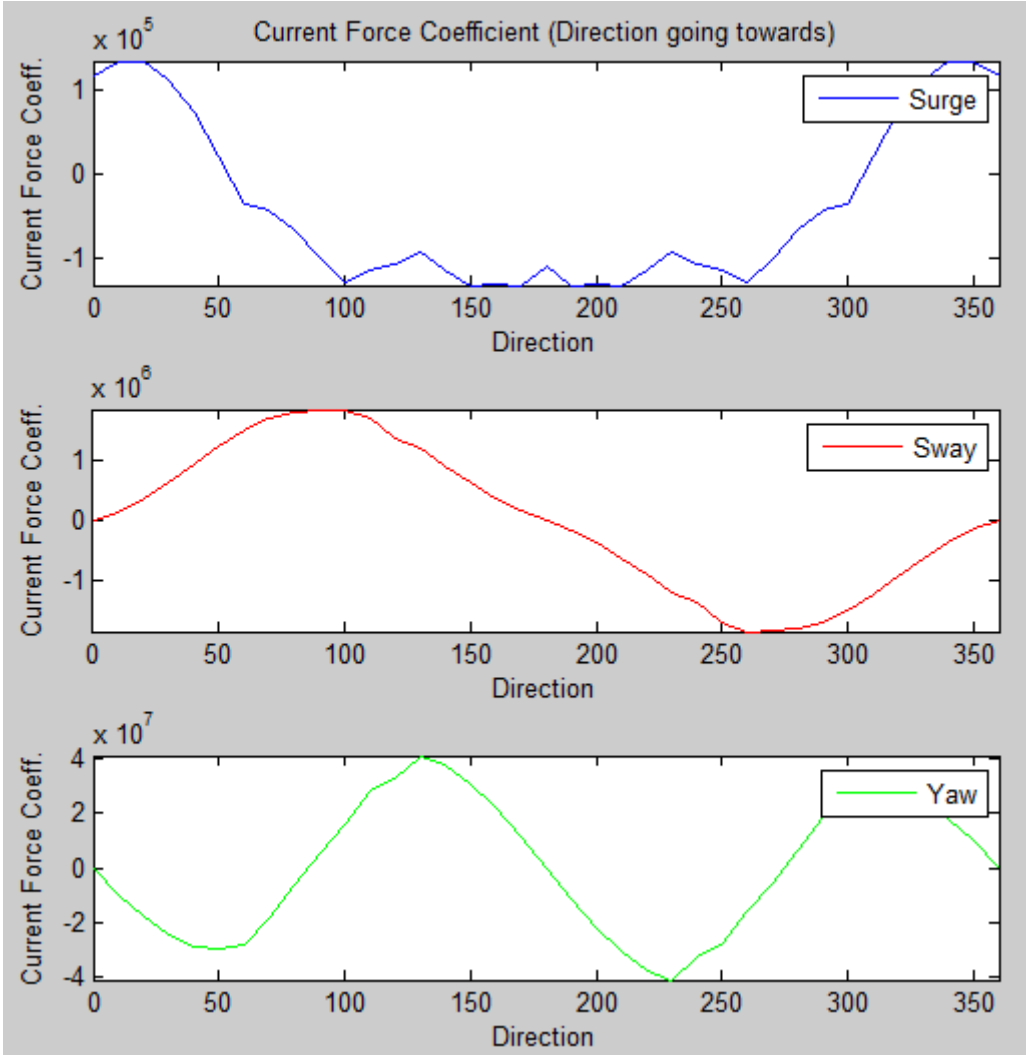


Figure: Plots for current coefficient for surge sway and yaw in all direction

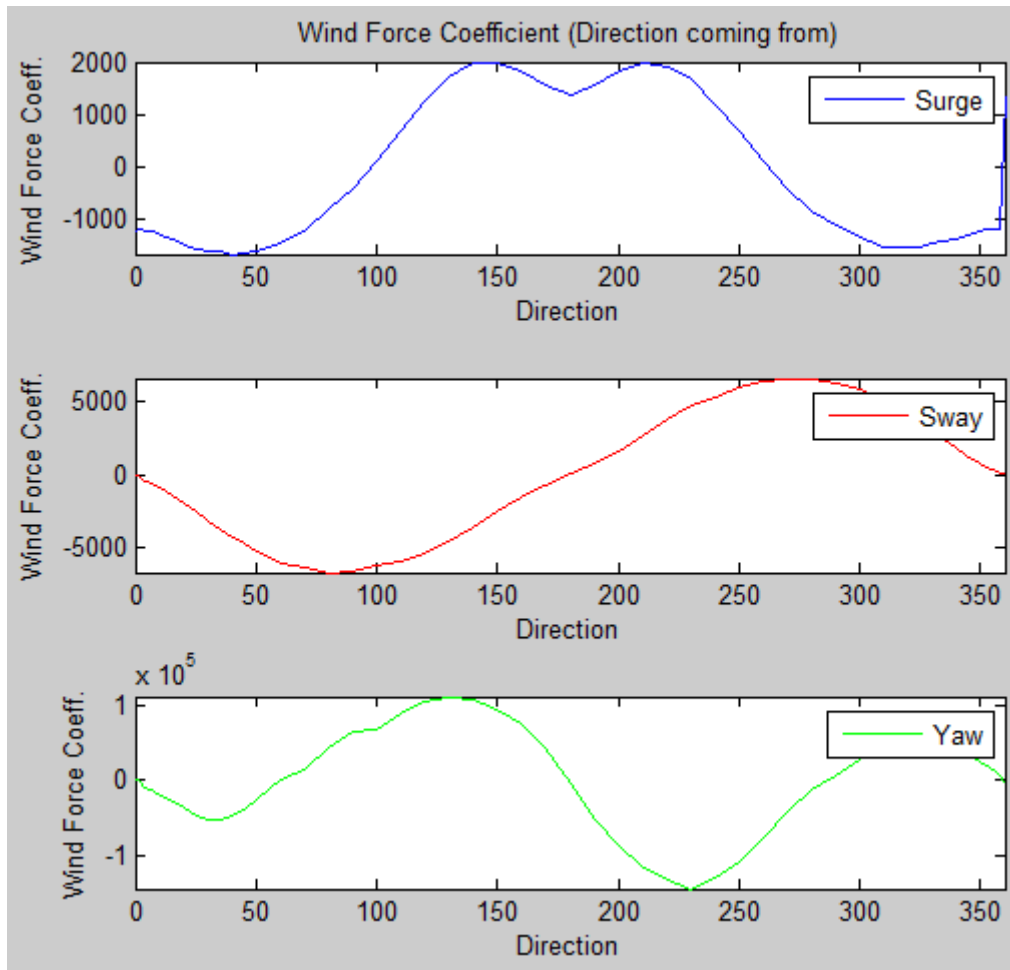


Figure: Plots for current coefficient for surge sway and yaw in all direction

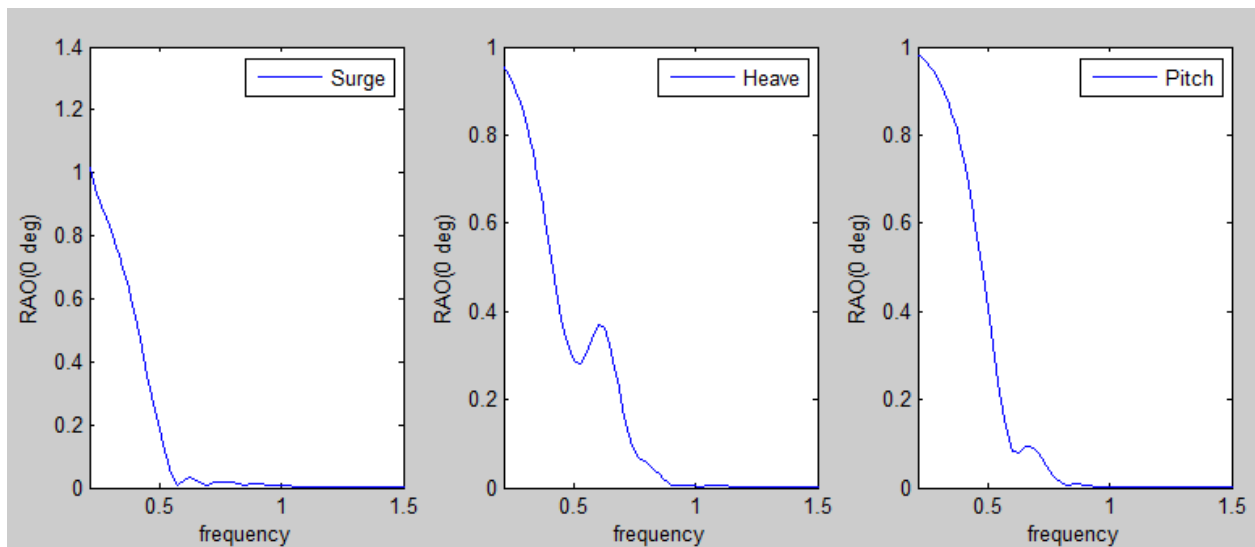


Figure: Plots for surge, heave and pitch for 0 degree heading

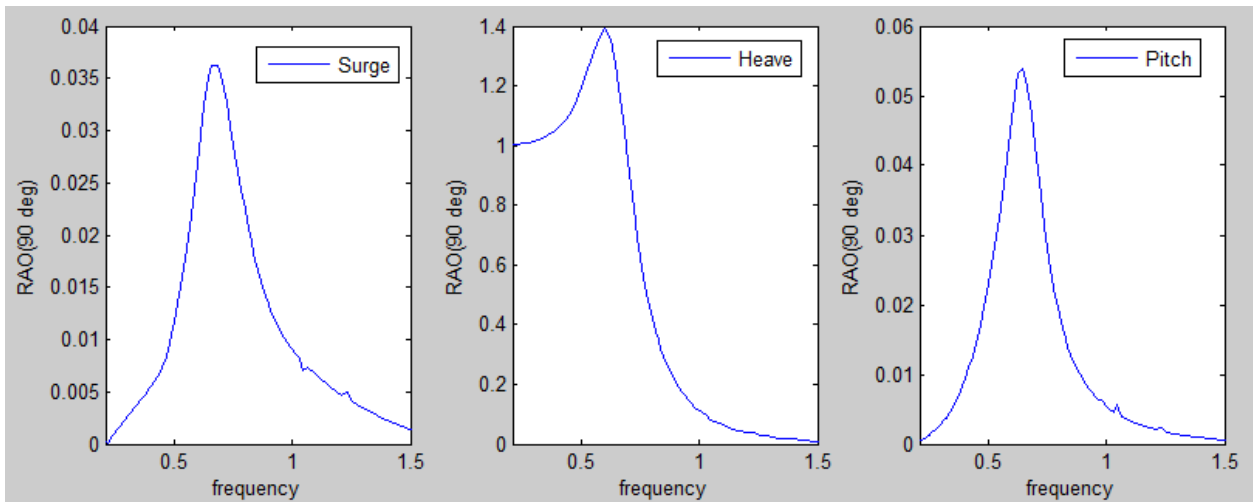


Figure: Plots for surge, heave and pitch for 90 degree heading

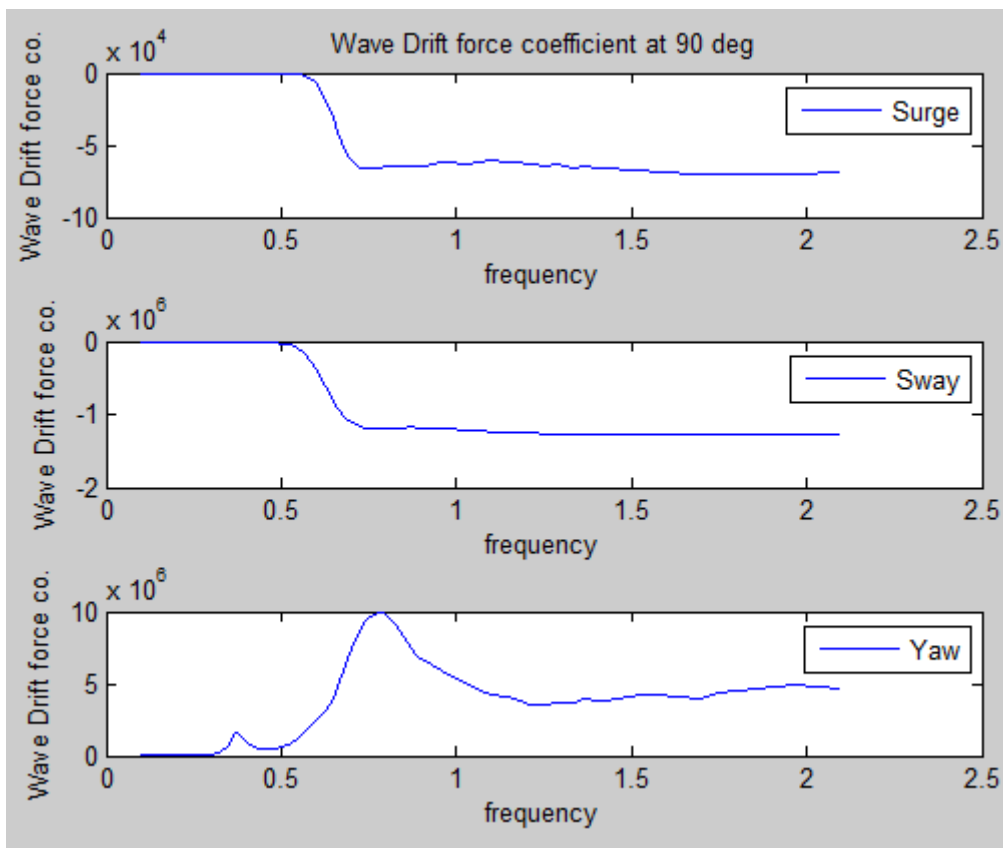


Figure: Plots for wave drift coefficient for 0 degree heading

APPENDIX E

Mathcad script for solving non-linear Weibull equation:

$D_k := 0.0504$ $DS := 358.69$ Guess Value (any constant)
 $n_o := 61958.78$ $h_{guess} := 1.0$
 $a := 6 \cdot 10^{10}$
 $m := 3$



Given

$$D(h) := \frac{n_o}{a} \cdot \frac{DS^m}{(\ln(n_o))^h} \cdot \Gamma\left(1 + \frac{m}{h}\right)$$

$$D(h_{guess}) = D_k$$

$$h := \text{Find}(h_{guess})$$



$$h = 0.666$$

$$D(h) = 0.05$$

APPENDIX F

Matlab script for getting vessel data from MIMOSA vessel file

```
% Script for reading MIMOSA vessel data file
clear all
close all
clc
    fid=fopen('Aasgard_Ball.txt','r');
        %Current force coefficient
    %Skipping the header file
for i=1:22      % i=1:(insert line no. which contains data 23100)
    fgetl(fid);
end
    %Gettin file
    Current=fscanf(fid,'%g',[8 37]);
    Current=Current';
    Current(:, 1)=[];
    Dir1 = Current(:, 1);
    Current(:, 1)=[];

    fclose(fid);
    %%
        % wind force coefficient
    fid=fopen('Aasgard_Ball.txt','r');
    for i=1:74      % i=1:(insert line no. which contains data 24100)
        fgetl(fid);
    end
    % Gettin file
    Wind=fscanf(fid,'%g',[8 55]);
    Wind=Wind';
    Wind(:, 1)=[];
    DirWind = Wind(:, 1);
    Wind(:, 1)=[];
    fclose(fid);
    %%
        % Frequencies for RAOs and Phases
    fid=fopen('Aasgard_Ball.txt','r');
    for i=1:131      % i=1:(insert line no. which contains data 30100)
        fgetl(fid);
    end
        A=fscanf(fid,'%g',[6 17]);
        A=A';
        A(:, 1)=[];
        A=A';
        j=1;
    for i=1:17
        f(j:j+4,1)=A(1:5,i);
        j=j+5;
    end
        Freq1=f(1:83,1);
        %RAOs and Phases
    for i=1:5
        fgetl(fid);
    end
    for i=1:6
        B = fscanf(fid,'%g',[3 83]);
        B=B';
        B(:, 1)=[];
        RAO(:,i)=B(:, 1);
```

```

        Phase(:,i)=B(:, 2);
end
fclose(fid);
%%
%Rao at 90 deg
fid=fopen('Aasgard_Ball.txt','r');

for i=1:3141      % i=1:(insert 1st line no. which contains data for RAO 90
deg)
    fgetl(fid);
end
for i=1:6
    G7 = fscanf(fid,'%g',[3 83]);
    G7=G7';
    G7(:, 1)=[];
    RAO90(:,i)=G7(:, 1);
    Phase90(:,i)=G7(:, 2);
end
fclose(fid);
%%
                                %Wave Drift coefficient

fid=fopen('Aasgard_Ball.txt','r');
%frequency for wave drift
for i=1:6629      % i=1:(insert line no. which contains data 40100)
    fgetl(fid);

end
C=fscanf(fid,'%g',[6 15]);
C=C';
C(:, 1)=[];
C=C';

Freq2=zeros(75,1);

j=1;
for i=1:15

    Freq2(j:j+4,1)=C(1:5,i);
    j=j+5;
end
%Heading for wave drift
Dir2 = 0:15:180;
Dir2 = Dir2';
%wave drift for 0 degree heading
for i=1:4
    fgetl(fid);
end
    WaveDrift = fscanf(fid,'%g',[7 75]);
    WaveDrift=WaveDrift';
    WaveDrift(:, 1)=[];

    fclose(fid);
    %wave drift for at 90 deg
    fid=fopen('Aasgard_Ball.txt','r');
for i=1:7097
    fgetl(fid);

end
    WaveDrift90 = fscanf(fid,'%g',[7 75]);

```

```

WaveDrift90=WaveDrift90';
WaveDrift90(:, 1)=[];

fclose(fid);

```

Matlab script for plotting

```

function createfigure(Tp1, Hs1, Prob1)
%CREATEFIGURE1(TP1, HS1, PROB1)
% TP1: surface xdata
% HS1: surface ydata
% PROB1: surface zdata
% Auto-generated by MATLAB on 24-May-2015 23:49:40
% Create figure
figure1 = figure;
% Create axes
axes1 = axes('Parent',figure1);
%% Uncomment the following line to preserve the X-limits of the axes
% xlim(axes1,[4 18]);
%% Uncomment the following line to preserve the Y-limits of the axes
% ylim(axes1,[1 13]);
view(axes1,[0.5 90]);
grid(axes1,'on');
hold(axes1,'all');
% Create title
title('Probability of sea states in Scatter diagram');
% Create xlabel
xlabel('Tp','VerticalAlignment','cap','HorizontalAlignment','center');
% Create ylabel
ylabel('Hs','VerticalAlignment','bottom','Rotation',90,...
'HorizontalAlignment','center');
% Create surf
surf(Tp1,Hs1,Prob1,'Parent',axes1);
% Create colorbar
colorbar('peer',axes1);

% script for plotting probability and fatigue damage in Matlab

createfigure1 (Tp,Hs,Prob);
title('Probability of sea states in Scatter diagram');

createfigure1 (Tp,Hs,dm1);
title('Calculated Damage of mooring line 1 using MIMOSA (p=0.156) ');

createfigure1 (Tp,Hs,dm7);
title('Calculated Damage of mooring line 7 using MIMOSA (p=0.156) ');

createfigure1 (Tp,Hs,ds1);
title('Calculated Damage of mooring line 1 using SIMA (p=0.156) ');

createfigure1 (Tp,Hs,ds7);
title('Calculated Damage of mooring line 7 using SIMA (p=0.156) ');

%% All plots
                                % current plots
F1=figure;
subplot(3,1,1);
plot(Dir1,Current(:,1));

```

```

xlabel('Direction');
ylabel('Current Force Coeff. ');
legend('Surge');
axis tight
title('Current Force Coefficient (Direction going towards)')
subplot(3,1,2);
plot(Dir1,Current(:,2),'r');
xlabel('Direction');
ylabel('Current Force Coeff. ');
legend('Sway');
axis tight
subplot(3,1,3);
plot(Dir1,Current(:,6),'g');
xlabel('Direction');
ylabel('Current Force Coeff. ');
legend('Yaw');
axis tight

                                % Wind plots
F1=figure;
subplot(3,1,1);
plot(DirWind,Wind(:,1));
xlabel('Direction');
ylabel('Wind Force Coeff. ');
legend('Surge');
axis tight
title('Wind Force Coefficient (Direction coming from)')
subplot(3,1,2);
plot(DirWind,Wind(:,2),'r');
xlabel('Direction');
ylabel('Wind Force Coeff. ');
legend('Sway');
axis tight
subplot(3,1,3);
plot(DirWind,Wind(:,6),'g');
xlabel('Direction');
ylabel('Wind Force Coeff. ');
legend('Yaw');
axis tight
    subplot(3,1,1);
plot(DirWind,Wind(:,1));
xlabel('Direction');
ylabel('Wind Force Coeff. ');
legend('Surge');
axis tight
title('Wind Force Coefficient (Direction coming from)')
subplot(3,1,2);
plot(DirWind,Wind(:,2),'r');
xlabel('Direction');
ylabel('Wind Force Coeff. ');
legend('Sway');
axis tight
subplot(3,1,3);
plot(DirWind,Wind(:,6),'g');
xlabel('Direction');
ylabel('Wind Force Coeff. ');
legend('Yaw');
axis tight

    %plot of RAO at 0 deg
F1=figure;
subplot(1,3,1);

```

```

plot(Freq1(:,1),RAO(:,1));
xlabel('frequency');
ylabel('RAO(0 deg)');
legend('Surge');
subplot(1,3,2);
plot(Freq1(:,1),RAO(:,3));
xlabel('frequency');
ylabel('RAO(0 deg)');
legend('Heave');
subplot(1,3,3);
plot(Freq1(:,1),RAO(:,5));
xlabel('frequency');
ylabel('RAO(0 deg)');
legend('Pitch');
%subplot(2,2,4);
%plot(Freq1(:,1),RAO(:,6));
%xlabel('frequency');
%ylabel('RAO(0 deg)');
%legend('Yaw');

                                %plot of RAO at 90 deg
F1=figure;
subplot(1,3,1);
plot(Freq1(:,1),RAO90(:,1));
xlabel('frequency');
ylabel('RAO(90 deg)');
legend('Surge');
subplot(1,3,2);
plot(Freq1(:,1),RAO90(:,3));
xlabel('frequency');
ylabel('RAO(90 deg)');
legend('Heave');
subplot(1,3,3);
plot(Freq1(:,1),RAO90(:,5));
xlabel('frequency');
ylabel('RAO(90 deg)');
legend('Pitch');
%subplot(2,2,4);
%plot(Freq1(:,1),RAO90(:,6));
%xlabel('frequency');
%ylabel('RAO(90 deg)');
%legend('Yaw');

                                %plot of Wave Drift force coefficient at 0 deg
F1=figure;
subplot(3,1,1);
plot(Freq2(:,1),WaveDrift(:,1));
xlabel('frequency');
ylabel('Wave Drift force co. ');
legend('Surge');
title('Wave Drift force coefficient at 0 deg');
subplot(3,1,2);
plot(Freq2(:,1),WaveDrift(:,2));
xlabel('frequency');
ylabel('Wave Drift force co. ');
legend('Sway');
subplot(3,1,3);
plot(Freq2(:,1),WaveDrift(:,6));
xlabel('frequency');
ylabel('Wave Drift force co. ');
legend('Yaw');

```



```
%plot of Wave Drift force coefficient at 90 deg
F1=figure;
subplot(3,1,1);
plot(Freq2(:,1),WaveDrift90(:,1));
xlabel('frequency');
ylabel('Wave Drift force co. ');
legend('Surge');
title ('Wave Drift force coefficient at 90 deg');
subplot(3,1,2);
plot(Freq2(:,1),WaveDrift90(:,2));
xlabel('frequency');
ylabel('Wave Drift force co. ');
legend('Sway');
subplot(3,1,3);
plot(Freq2(:,1),WaveDrift90(:,6));
xlabel('frequency');
ylabel('Wave Drift force co. ');
legend('Yaw');
```